Received: 29 May 2021 | Revised: 27 September 2021 | Accepted: 1 January 2022

DOI: 10.1111/apha.13777

ACTA PHYSIOLOGICA

REGULAR PAPER

A novel K^+-dependent Na^+ uptake mechanism during low pH exposure in adult zebrafish (*Danio rerio*): New tricks for old dogma

Alexander M. Clifford[1,2] | **Martin Tresguerres**[2] | **Greg G. Goss**[3] | **Chris M. Wood**[1]

[1]Department of Zoology, University of British Columbia, Vancouver, British Columbia, Canada

[2]Marine Biology Research Division, Scripps Institution of Oceanography, University of California San Diego, La Jolla, California, USA

[3]Department of Biological Sciences, University of Alberta, Edmonton, Alberta, Canada

Correspondence
Alexander M. Clifford, Scripps Institution of Oceanography, University of California San Diego, 8750 Biological Grade, Hubbs Hall 3120, La Jolla, CA 92037.
Email: alex.clifford@me.com

Funding information
AMC was supported by a Natural Sciences and Engineering Research Council (NSERC) Discovery grant awarded to CMW (RGPIN-2017-03843), and a Scripps Institution Oceanography Postdoctoral Research Scholar Fellowship. MT provided SIO discretionary funds and was funded by the National Science Foundation (IOS# 1754994). GGG was funded by NSERC (RGPIN-2016-04678).

Abstract

Aim: To determine whether Na^+ uptake in adult zebrafish (*Danio rerio*) exposed to acidic water adheres to traditional models reliant on Na^+/H^+ Exchangers (NHEs), Na^+ channels and Na^+/Cl^- co-transporters (NCCs) or if it occurs through a novel mechanism.

Methods: Zebrafish were exposed to control (pH 8.0) or acidic (pH 4.0) water for 0-12 hours during which $^{22}Na^+$ uptake (J^{Na}_{in}), ammonia excretion, net acidic equivalent flux and net K^+ flux (J^{H}_{net}) were measured. The involvement of NHEs, Na^+ channels, NCCs, K^+-channels and K^+-dependent Na^+/Ca^{2+} exchangers (NCKXs) was evaluated by exposure to Cl^--free or elevated $[K^+]$ water, or to pharmacological inhibitors. The presence of NCKXs in gill was examined using RT-PCR.

Results: J^{Na}_{in} was strongly attenuated by acid exposure, but gradually recovered to control rates. The systematic elimination of each of the traditional models led us to consider K^+ as a counter substrate for Na^+ uptake during acid exposure. Indeed, elevated environmental $[K^+]$ inhibited J^{Na}_{in} during acid exposure in a concentration-dependent manner, with near-complete inhibition at 10 mM. Moreover, J^{H}_{net} loss increased approximately fourfold at 8-10 hours of acid exposure which correlated with recovered J^{Na}_{in} in 1:1 fashion, and both J^{Na}_{in} and J^{H}_{net} were sensitive to tetraethylammonium (TEA) during acid exposure. Zebrafish gills expressed mRNA coding for six NCKX isoforms.

Conclusions: During acid exposure, zebrafish engage a novel Na^+ uptake mechanism that utilizes the outwardly directed K^+ gradient as a counter-substrate for Na^+ and is sensitive to TEA. NKCXs are promising candidates to mediate this K^+-dependent Na^+ uptake, opening new research avenues about Na^+ uptake in zebrafish and other acid-tolerant aquatic species.

KEYWORDS

ionoregulation, low pH, Na^+/Ca^{2+}-K^+ exchanger, Na^+/H^+ exchanger, Na^+-Cl^- cotransporter, sodium uptake

© 2022 Scandinavian Physiological Society. Published by John Wiley & Sons Ltd

1 | INTRODUCTION

Freshwater teleosts are faced with the challenge of diffusive ion loss to their hypo-osmotic surroundings and thus actively take up Na^+ from the environment. The current dogma for freshwater fish gills proposes three Na^+ uptake mechanisms within ion transporting cells (ionocytes): (a) August Krogh's classic apical Na^+/H^+ (NH_4^+) exchange,[1–3] (Figure 1A) mediated by Na^+/H^+ exchangers (NHEs) and possibly augmented by outward transport of NH_3 by Rhesus (Rh) glycoproteins,[4–7] (b) uptake through, as of yet unidentified, apical Na^+ channel(s) (Figure 1B) or related acid-sensing ion channel(s) (ASICs)[8,9] electrogenically coupled to apical H^+ excretion via V-H^+-ATPase (VHA),[10–12] and more recently (c) co-transport of Na^+ and Cl^- via Na^+/Cl^- co-transporters (NCCs; Figure 1C).[13] These molecular mechanisms are analogous to apical Na^+-reabsorption mechanisms in the mammalian kidney where roughly two-thirds of Na^+ reabsorption occurs by proximal tubule NHEs and the remainder is mediated by NCCs and epithelial Na^+ channels (ENaCs) in the distal convoluted tubules and collecting ducts respectively.[14–16]

Abundant evidence suggests that Na^+ uptake via NHE is the prevalent mechanism in freshwater teleosts[17–19]; however, uptake solely via NHE relies on thermodynamically favourable conditions.[20] The operational direction of NHE is fundamentally dictated by environmental and intra-ionocyte concentration gradients of Na^+ and H^+, such that Na^+ uptake is favoured only when

$$\frac{[Na^+]_i}{[Na^+]_o} < \frac{[H^+]_i}{[H^+]_o} \quad (1)$$

At low environmental [Na^+] or pH (ie high [H^+]), NHE will function in the direction of Na^+ excretion, to the detriment of Na^+ homeostasis.[10,20] However, many freshwater fishes can still live in low pH and/or low [Na^+] water where NHE should not function. For example wild zebrafish (*Danio rerio*) have been observed in shallow streams with pH < 6.0,[21] and their natural habitat includes stagnant ponds and rice paddies that can be even more acidic (as low as pH 3.5) because of acidic soils or agricultural runoff.[22–26] Furthermore, zebrafish are known to aggregate in very dense shoals, which likely results in additional acidification.[27] Indeed, zebrafish are quite tolerant of acidic environments, and capable of long-term (>2 weeks) survival in waters as low as pH 4.0.[28] Stimulations of Na^+ uptake by larval zebrafish in response to acid exposure have been reported,[29,30] suggesting the involvement of mechanisms other than NHE.

One proposed solution to overcoming the thermodynamic constraints on Na^+ uptake by NHE at low external pH is by forming a functional metabolon with Rhcg (Rh glycoprotein type c; a purported NH_3 channel[31]), whereby Rhcg strips H^+ from NH_4^+ and transports NH_3 across the membrane, thereby generating a H^+ driving gradient powering NHE in the Na^+ uptake direction (Figure 1A). Once outside, NH_3 is re-protonated to NH_4^+, thus maintaining the outwardly directed NH_3 gradient while simultaneously raising the local boundary layer pH so that NHE function in the Na^+ uptake direction is further favoured.[4] In support of this hypothesis, translational knockdown of either Rhcg1 or NHE3b in larval zebrafish resulted in an attenuation of stimulated Na^+ uptake in acid-reared zebrafish.[29] However, it remains unclear if the NHE/Rhcg metabolon could function at extremely low pHs, or even if it is functional in adult zebrafish.

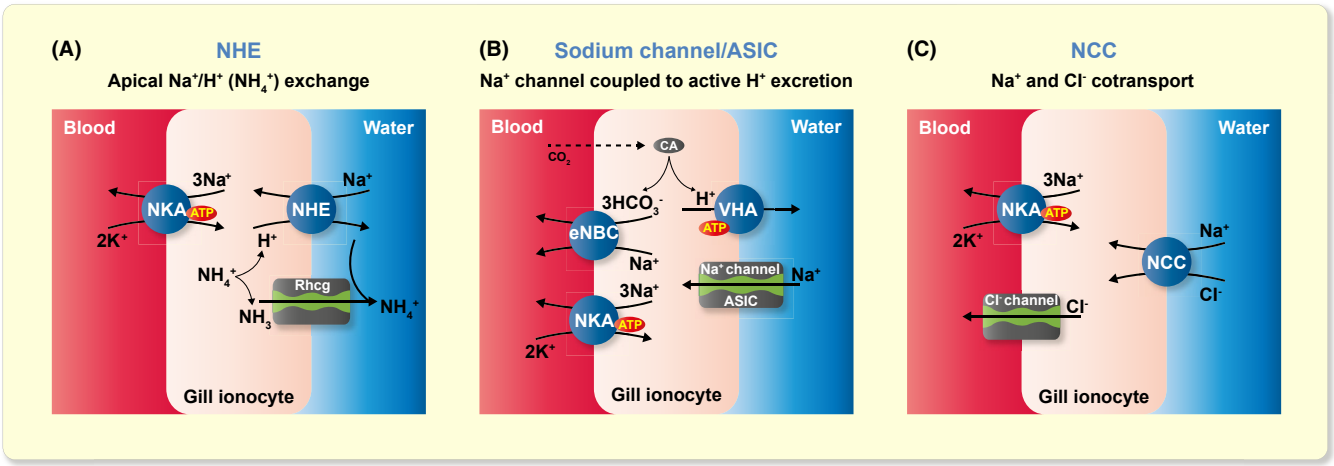

FIGURE 1 Putative models for Na^+ uptake in freshwater fishes. (A) August Krogh's classic apical Na^+/H^+ (NH_{4+}) exchange mediated by Na^+/H^+ Exchangers (NHEs), possibly in combination with Rhesus (Rh) glycoproteins, (B) apical Na^+ channels and/or acid-sensing ion channels (ASIC) electrogenically coupled to apical proton excretion via V-H^+-ATPase (VHA), (C) coupled uptake with Cl^- via Na^+/Cl^- co-transporters (NCC)

In an alternative mechanism, Na^+ uptake in adult zebrafish and rainbow trout (*Oncorhynchus mykiss*) held in very low (<0.1 mM) environmental [Na^+] seems to be mediated primarily by ASICs electrogenically coupled to apical proton excretion via VHA, rather than via NHEs. In both fish species, amiloride-insensitive Na^+ uptake was inhibited by the ASIC-inhibitor DAPI (4′,6-diamidino-2-phenylindole),[8,9] and in zebrafish, Na^+ uptake persisted despite NHE3b knockout via CRISPr/Cas9 deletion.[32] However, it is not known whether this mechanism is also functional during exposure to low pH conditions.

Finally, uptake of Na^+ by zebrafish during acid exposure may be mediated by apical Na^+/Cl^- cotransporters (NCCs). The supporting evidence includes an increased abundance of gill NCC cells and decreased expression of *nhe3b*/NHE3b following exposure of adult zebrafish to low pH environments (2-7 days). In addition, zebrafish larvae exposed to similar conditions demonstrated an increased abundance of skin NCC cells, enlarged NCC cells and increased *ncc* mRNA expression.[33] In another study, zebrafish larvae pre-exposed to pH 4.0 for 2 hours demonstrated increased Na^+ and Cl^- influx upon return to circumneutral pH. The uptake of each ion was attenuated when the other ion was omitted from the water (ie Cl^--free and Na^+-free conditions respectively) as well as upon NCC morpholino knockdown; however, VHA knockdown had no effect.[13] A major caveat is that these flux measurements were performed in circumneutral pH water, and therefore evaluated the role of NCC during recovery from acute acid exposure and not necessarily the mechanism responsible for Na^+ uptake during exposure to acidic conditions. Moreover, in low [Na^+] trials, removal of water Cl^- (to inhibit potential rescue by a putative NCC mechanism) combined with VHA morpholino knockdown in the NHE3b knockout zebrafish all failed to reduce Na^+ uptake.[32] Finally, in the proposed model, both [Na^+] and [Cl^-] in the water are multiple orders of magnitude lower than nominal intracellular concentrations, raising questions about how NCC transport could be energized. These observations point to a novel, as of yet undescribed mechanism for Na^+ uptake in zebrafish in very low [Na^+] and/or very low pH environments and in this lies the impetus for the current study.

Our goal was to characterize the acid-inducible Na^+ uptake mechanism in zebrafish by analysis of the recovery of Na^+ uptake during continued acid exposure. We hypothesized that acute exposure to low pH (pH 4.0) conditions would inhibit NHE function because of adverse ion motive gradients.[20] Radio-labelled ^{22}Na was used to measure the return of unidirectional Na^+ uptake flux rates (J^{Na}_{in}) during exposure, allowing us to characterize the upregulation of alternate Na^+ uptake mechanisms. Through a series of flux studies utilizing putative drug inhibitors (Table 1), ion-replacement, and kinetic analyses, we ruled out contributions from the previously proposed Na^+ uptake mechanisms, and

TABLE 1 List of inhibitors and their putative targets

Drug	IUPAC name	[Drug]	Target notes	References
Amiloride	3,5-diamino-6-chloro-N-(diaminomethylene) pyrazine-2-carboxamide	200 μM	NHE, ENaC, ASIC	9,34,35
DAPI	2-(4-Amidinophenyl)-1*H*-indole-6-carboxamidine	20 μM	ASIC, possibly NHE2	8,9,36,37
EIPA	5-(N-Ethyl-N-isopropyl)amiloride	50 μM	NHE	9,29,34,37,38
Phenamil	3,5-Diamino-6-chloro-N-(N-phenylcarbamimidoyl)-2-pyrazinecarboxamide	50 μM	ENaC	34,39–41
Bumetanide	3-butylamino-4-phenoxy-5-sulfamoyl-benzoic acid	100 μM	NKCC	37,42
Hydrochlorothiazide	6-chloro-1,1-dioxo-3,4-dihydro-2*H*-1,2,4-benzothiadiazine-7-sulfonamide	100 μM	NCC	37,43
Metolazone	7-chloro-2-methyl-4-oxo-3-o-tolyl-1,2,3,4-tetrahydroquinazoline-6-sulfonamide	100 μM	NCC	44–46
Acetazolamide	5-acetamido-1,3,4-thiadiazole-2-sulfonamide	100 μM	CA	10,47
Barium	$BaCl_2$	10 mM	Broad spectrum K^+ channel inhibitor	48–51
4-Aminopyridine	Pyridin-4-amine	500 μM	Kv1 channels Ca^{2+}-activated K^+ channels	52
Tetraethylammonium	tetraethylazanium	1 mM	K^+ channels (Ca^{2+} activated, Voltage gated), NKA, NCKX	53–58

uncovered evidence for a thus far unreported Na^+ uptake mechanism that is electroneutrally linked to outward K^+ movement. This newly identified Na^+ uptake mechanism operates to rescue Na^+ uptake during exposure to low environmental pH.

2 | RESULTS

2.1 | Series 1: Time-course dynamics of zebrafish ion-regulatory status during acid exposure

Zebrafish were exposed to either control (pH ~8.0) or acid (pH 4.0) conditions for up to 12 hours while ion flux components were characterized intermittently throughout; pH 4.0 was chosen for the acid exposure based on range-finder tests (see Section 4; Series 1). In zebrafish exposed to control pH conditions, Na^+ uptake ($J^{Na}{}_{in}$) remained statistically unchanged throughout the course of exposure (Figure 2A). Upon initial acid exposure, $J^{Na}{}_{in}$ dropped precipitously by 75% within the first hour and remained significantly lower than pairwise control zebrafish throughout the first 8 hours of exposure ($P < .05$), but returned to levels not significantly different from pairwise control zebrafish at 8-10 hours ($P = .9997$) and 10-12 hours ($P = .4101$).

In addition to $J^{Na}{}_{in}$, we concurrently measured ammonia excretion ($J^{amm}{}_{net}$) and titratable acidity minus bicarbonate ($J^{TA-HCO_3^-}$). These were summed together to yield net acid excretion $J^{H}{}_{net}$ (acid equivalent excretion denoted by negative values; base equivalent excretion denoted by positive values) to evaluate potential contributing roles of an NHE-Rh mediated mechanism and/or a VHA-linked ASIC/Na^+ channel mechanism in the aforementioned restoration of $J^{Na}{}_{in}$ during acid exposure. $J^{amm}{}_{net}$ averaged ~840 nmol g^{-1} $hour^{-1}$ and remained relatively unchanged throughout the time series in zebrafish held in control pH conditions (Figure 2B; $P > .9514$). Compared to pairwise controls, $J^{amm}{}_{net}$ in acid-exposed zebrafish significantly increased only for 0-1 hours of exposure (approximately threefold higher, $P = .0278$) and returned to control levels throughout the remainder of the time series. No significant effects of time or treatment were noted in either $J^{TA-HCO_3^-}$ (Figure 2C) or $J^{H}{}_{net}$ (Figure 2D) ($F_{6,68} < 2.906$, $P > .0928$), indicating a lack of net acid-base disturbances at all time periods and treatments.

2.2 | Series 2: Pharmacological profile of the re-established Na^+ uptake mechanism during acid exposure

We measured $J^{Na}{}_{in}$ in zebrafish (a) during exposure to control pH water, (b) for 0-2 hours exposure to pH 4.0

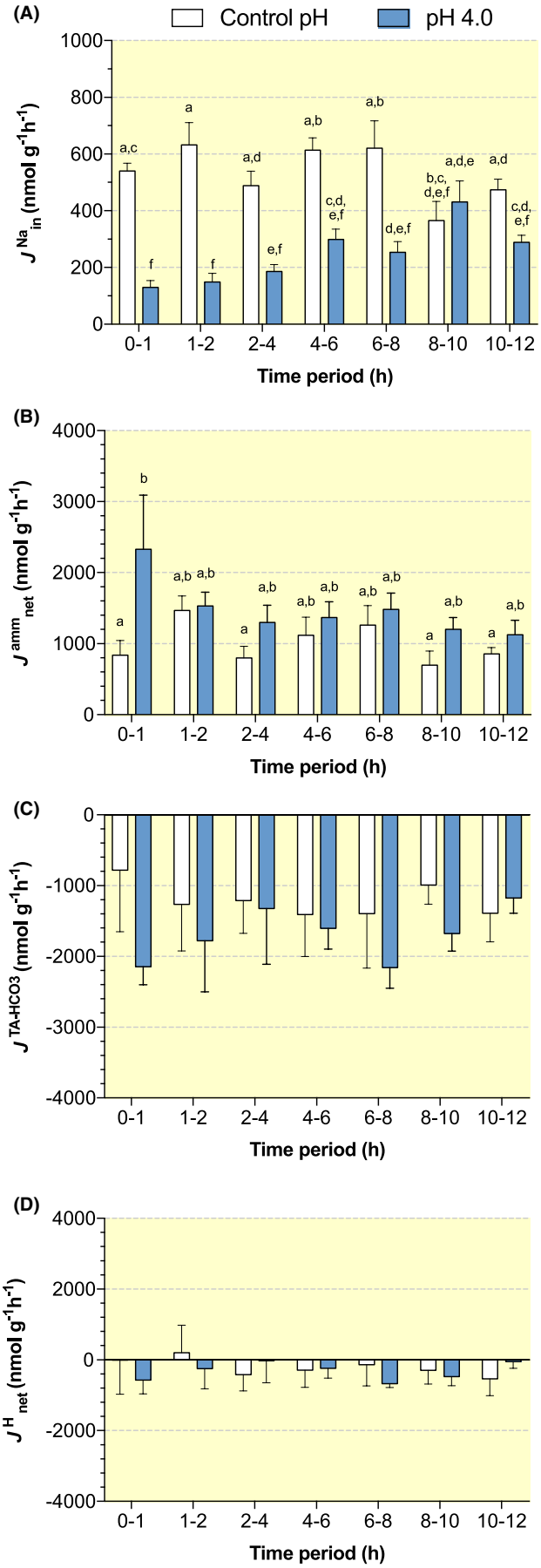

FIGURE 2 Time-dependent dynamics of zebrafish ion regulation during low pH exposure. Groups of zebrafish were held in either control pH conditions (pH 8.0; white bars) or acidic water (pH 4.0; blue bars) for up to 12 h, and individuals (n = 6) were removed to determine (A) rates of Na^+ uptake ($J^{Na}{}_{in}$) via ^{22}Na appearance into the animal and (B) net ammonia excretion ($J^{amm}{}_{net}$) over 1-2 hour periods. Throughout the time series, (C) $J^{TA-HCO_3^-}$ (flux of titratable acidity minus HCO_3^-; base equivalent excretion denoted by negative values, acid excretion denoted by positive values) was also characterized. Respective $J^{TA-HCO_3^-}$ values were added to $J^{amm}{}_{net}$ values to calculate (D) $J^{H}{}_{net}$ (excretion rates of net H^+ equivalents). Data are presented as mean ± SE. Data not sharing letters denote significant differences (two-way ANOVA; Tukey's post hoc test making all comparisons; n = 6, $P < .05$)

and (c) for 8-10 hours exposure to pH 4.0. During these flux treatments, zebrafish were concurrently exposed to a panel of pharmacological inhibitors (Table 1) targeting key transporters either directly or indirectly involved in Na^+ uptake (Figure 3). The general trend observed in vehicle control zebrafish (0.05% DMSO) was a robust $J^{Na}{}_{in}$ uptake during control pH conditions, a reduction in $J^{Na}{}_{in}$ during immediate acid exposure [significant in trial set (a) and (c), with a non-significant reduction in trial set (b)], and a general return to control rates during acid exposure after 8 hours pre-exposure. Of all drugs tested, $J^{Na}{}_{in}$ was sensitive only to amiloride and EIPA, and only during control pH exposure; $J^{Na}{}_{in}$ in either case was inhibited by 60%-70% compared to vehicle controls. Interestingly, the reductions in $J^{Na}{}_{in}$ were comparable to those caused by acute exposure (0-2 hours) to pH 4.0 (Figure 2A), and neither amiloride nor EIPA caused any further inhibition relative to the respective vehicle control zebrafish at either 0-2 or 8-10 hours of continuing acid exposure. No other differences of note were observed across all other treatments or drugs (ie DAPI [Figure 2A], phenamil, hydrochlorothiazide and bumetanide [Figure 2B], as well as metolazone and acetazolamide [Figure 3C]).

2.3 | Series 3: Investigating the role of Cl^- in the re-establishment of $J^{Na}{}_{in}$ during and after acid exposure

To test for a possible linkage between the restoration of $J^{Na}{}_{in}$ and environmental Cl^-, we characterized $J^{Na}{}_{in}$ in two separate exposure/flux protocols, (a) in control pH water after 0, 2, or 8 hr of pre-exposure to pH 4.0 (Figure 4A), and (b) in each of the three treatments described in Series 2 (ie control pH and pH 4.0 at 0-2 hours, and pH 4.0 at 8-10 hours; Figure 4B). In both protocols, $J^{Na}{}_{in}$ was measured either in Cl^--containing or Cl^--free flux media.

In zebrafish transferred from control holding conditions, removal of environmental Cl^-elicited no significant differences in $J^{Na}{}_{in}$ when characterized in control pH conditions (Figure 4A; $P = .1813$). Furthermore, $J^{Na}{}_{in}$ in zebrafish pre-exposed to acidic conditions for 2 and 8 hours were not significantly different from 0 hour rates in Cl^--containing media ($P > .9346$), nor were differences in $J^{Na}{}_{in}$ detected between the two lengths of acid exposure ($P = .9804$). Interestingly, we did note a significant time-dependent increase in $J^{Na}{}_{in}$ in Cl^--free trials whereby 8 hours pre-exposed zebrafish exhibited approximately twofold increase in $J^{Na}{}_{in}$ compared to the 0 hours control zebrafish fluxed in the same Cl^--free medium (Figure 4A; $P = .0023$).

When $J^{Na}{}_{in}$ was characterized according to the treatments described in Series 2, $J^{Na}{}_{in}$ in both Cl^--containing and Cl^--free conditions followed the same inhibition and recovery patterns (Figure 4B) seen in Series 1 and Series 2 (ie Figures 2A and 3). $J^{Na}{}_{in}$ patterns were statistically unchanged between Cl^--containing and Cl^--free conditions; an effect of Cl^--free media was not observed ($P > .6807$).

2.4 | Series 4: Investigating the role of environmental $[K^+]_o$ in the re-established Na^+ uptake mechanism during acid exposure

Zebrafish were exposed to the aforementioned treatments in either high environmental K^+ (HEK; 50 mM K^+ as 25 mM K_2SO_4) or in K^+-free medium (50 mM NMDG-Cl as elevated [Cl^-] control). Zebrafish in K^+-free conditions generally displayed similar pH-dependent inhibition and time-dependent recovery pattens (Figure 5A) to those observed in previous experimental series (Figures 2A, 3 and 4B): a significant reduction (~60%) in $J^{Na}{}_{in}$ during initial (0-2 hours) pH 4.0 exposure ($P = .0092$), followed by a recovery in $J^{Na}{}_{in}$ for 8-10 hours of pH 4.0 exposure that was not significantly different from $J^{Na}{}_{in}$ in control pH exposed zebrafish ($P = .9756$). While HEK elicited no effects on $J^{Na}{}_{in}$ during exposure to control pH conditions ($P = .9258$), HEK during initial pH 4.0 exposure caused an even greater inhibition of $J^{Na}{}_{in}$ compared to rates measured during control pH exposure (~95% inhibition; $P < .0001$), well below (~85%) the rates observed during initial pH 4.0 exposure in K^+-free conditions ($P < .0007$). Furthermore, HEK also significantly impacted the recovery of $J^{Na}{}_{in}$ following prolonged (8-10 hours) pH 4.0 exposure; $J^{Na}{}_{in}$ remained significantly depressed compared to rates observed in control pH media (~90% reduction, $P < .0001$).

The $J^{K}{}_{net}$ observed in K^+-free conditions in control pH and after immediate exposure to pH 4.0 (0-2 hours) were

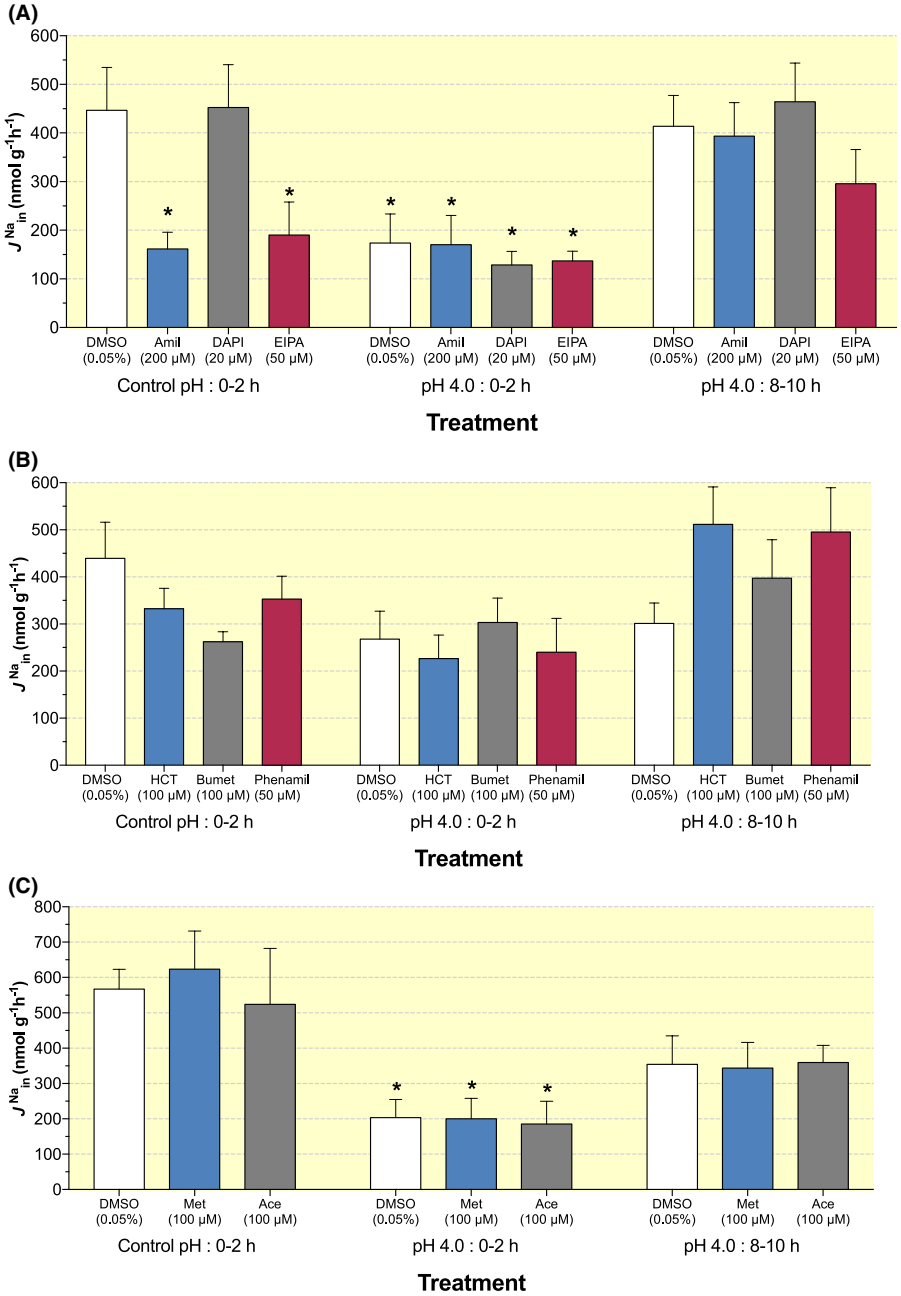

FIGURE 3 Effect of pharmacological inhibitors on J^{Na}_{in} in zebrafish during acid exposure. J^{Na}_{in} was determined in control pH (pH 8.0) or pH 4.0 conditions acutely (0-2 h) or pH 4.0 conditions following 8 hours of acid exposure. Thirty minutes prior to the addition of ^{22}Na, zebrafish were first incubated in flux-media containing (A) Amiloride (Amil; 200 μM), DAPI (20 μM) and EIPA (50 μM), (B) Hydrochlorothiazide (HCT; 100 μM), Bumetanide (Bumet; 100 μM) and Phenamil (50 μM), (C) Metolazone (Met; 100 μM) and Acetazolamide (Ace; 100 μM); Vehicle controls (DMSO; 0.05%) were conducted for each drug panel (white bars). Data are presented as mean ± SE. Data presented with asterisks (*) denote significant differences from Control pH:0-2 h/DMSO treatment (two-way ANOVA; Dunnett's post hoc test against control groups measured during control pH conditions in DMSO spiked flux media; n = 6, $P < .05$)

negative and not significantly different from each other (Figure 5B), indicating a small net loss from the animal. However, zebrafish that had been exposed to pH 4.0 for 8-10 hours had approximately fourfold increase in outwardly directed J^{K}_{net}. Furthermore, linear regression analysis of outwardly directed J^{K}_{net} vs inwardly directed J^{Na}_{in} in zebrafish exposed to pH 4.0 for 8-10 hours demonstrated a solid 1:1 correlation [($R^2 = 0.9732$; slope not significantly different than 1.0 ($F_{1,4} = 0.5872$, $P = .4862$)] (Figure 5C). This 1:1 relationship was further substantiated in a more robust linear regression analysis involving all paired J^{K}_{net} and J^{Na}_{in} observations from zebrafish which were subject to prolonged (8-10 hours) pH 4.0 exposure in Series 4 (K^+-free zebrafish), Series 5 (all zebrafish), and Series 6 (NMDG- and DMSO-control zebrafish) [($R^2 = 0.7073$; slope not significantly different than 1.0 ($F_{1,44} = 0.5042$, $P = .4814$)] (Figure 5D).

J^{Na}_{in} was measured in zebrafish from each of the three treatments (control pH and pH 4.0 at 0-2 hours, pH 4.0 at 8-10 hours) in increasing environmental $[K^+]_o$ between 38.4 μM and 50 mM. During control pH exposure, there was no correlation between J^{Na}_{in} and environmental $[K^+]_o$, with a slope that did not differ significantly from 0 ($R^2 = 0.0132$; $F_{1,40} = 1.116$, $P = .2972$) (Figure 5E inset). In contrast, J^{Na}_{in} measured in both of the pH 4.0 exposures displayed clear concentration-dependent relationships with increasing reductions in J^{Na}_{in} at higher environmental $[K^+]_o$ (Figure 5E). J^{Na}_{in} data measured across

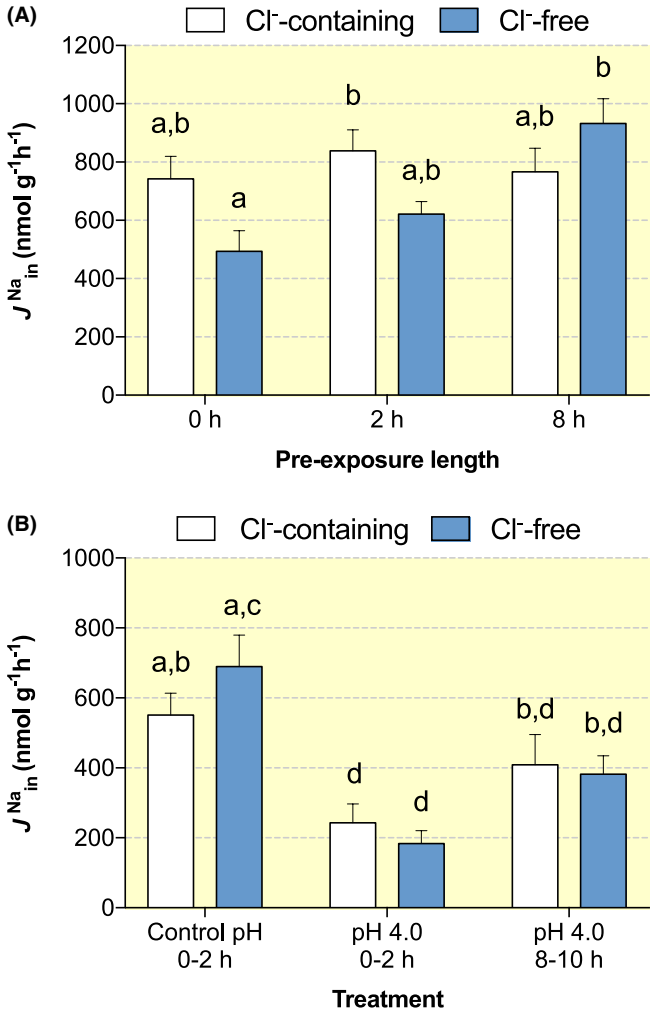

FIGURE 4 Effect of environmental Cl^- in the re-establishment of J^{Na}_{in} during and after acid exposure. Zebrafish were held in either control pH (pH 8.0) or acidic conditions (pH 4.0) for up to 8 hours prior to the measurement of J^{Na}_{in}. In (A) all J^{Na}_{in} measurements were made in control pH conditions. J^{Na}_{in} was determined in fish held in either Cl-free (blue bars) or Cl^--containing water (white bars) either before (0 hour pre-treatment control) or immediately after return to control pH conditions after 2 or 8 hours of acid exposure. In (B), measurements were either in Cl-free (blue bars) or Cl^--containing water (white bars) at the indicated pH and time period. Data are presented as mean + SE. Data not sharing letters denote significant differences (two-way ANOVA; Tukey's post hoc test making all comparisons; n = 6, $P < .05$)

increasing environmental $[K^+]_o$ were fitted to single-phase exponential curves and subsequently tested against one another. This analysis demonstrated that the half-life constant (interpreted as a proxy to K_i; the exposure concentration of K^+ that causes 50% inhibition of J^{Na}_{in}) was significantly greater in the prolonged acid exposure ($[K^+]_o$ = 1.468 mM) compared to acute acid exposure ($[K^+]_o$ = 0.5757 mM; $F_{1,90} = 4.999$, $P = .0278$).

2.5 | Series 5: Profiling the influence of environmental Na^+ on the dynamics of J^{Na}_{in} and J^{K}_{net} during acid exposure

The influence of environmental Na^+ concentration ($[Na^+]_o$) on the apparent Na^+ influx vs K^+ efflux mechanism was evaluated by changing $[Na^+]_o$ over a geometric series during control pH conditions and for 8-10 hours of acid exposure. These J^{K}_{net} and J^{Na}_{in} data were evaluated against linear and Michaelis-Menten models and the most appropriate fit was determined for each treatment. Michaelis-Menten patterns for saturable concentration-dependence of J^{Na}_{in} on $[Na^+]_o$ were observed both in zebrafish during control pH conditions and in zebrafish exposed to pH 4.0 for 8-10 hours (Figure 6A). In comparing these patterns, we observed significant differences in J_{max} (453.0 ± 96.3 nmol g^{-1} $hour^{-1}$ in control pH conditions vs 925.8 ± 148.2 nmol g^{-1} $hour^{-1}$ in pH 4.0 conditions) and K_m (75.8 ± 71.7 μM in control pH conditions vs 391.8 ± 151.4 μM in pH 4.0 conditions) ($F_{2,56} = 3.959$, $P = .0246$).

We also analysed J^{K}_{net} patterns in the same experimental series (Figure 6B). J^{K}_{net} in zebrafish tested during control pH conditions remained stable over all $[Na^+]_o$ levels along a line with a slope that was not significantly different from zero ($R^2 = 0.1094$; $F_{1,28} = 3.441$, $P = .0742$). However, zebrafish that had been pre-exposed to pH 4.0 for 8 hours demonstrated a clear $[Na^+]_o$-dependent K^+ efflux pattern [J^{K}_{net} (nmol K^+ g^{-1} $hour^{-1}$) = 302.2 ± 58.65 × $[Na^+]_o$ mM +143 ± 36.91; $R^2 = 0.2505$; $F_{1,27} = 26.55$. $P = .0001$].

2.6 | Series 6: Effect of K^+ transporter inhibitors on the re-established Na^+ uptake mechanism during acid exposure

In experimental protocols that mirrored Series 2, J^{Na}_{in} and J^{K}_{net} rates were measured in the presence of various K^+ channel inhibitors. NMDG control zebrafish and DMSO control zebrafish displayed similar J^{Na}_{in} acid-induced inhibition and recovery patterns as in previous experiments (Figure 7A,C), along with similar stimulation in J^{K}_{net} efflux following pre-exposure to pH 4.0 for 8 hours (Figure 7B,D). Curiously, in this experimental series, a non-significant stimulation of J^{K}_{net} efflux was also observed in NMDG control zebrafish fluxed immediately in pH 4.0 water, (Figure 7B). Ba^{2+} did not elicit any significant changes in either J^{Na}_{in} or J^{K}_{net} within the control pH treatment (Figure 7A,B) or during either acute or prolonged acid exposure in relation to measurements in NMDG-exposed zebrafish during control pH exposure.

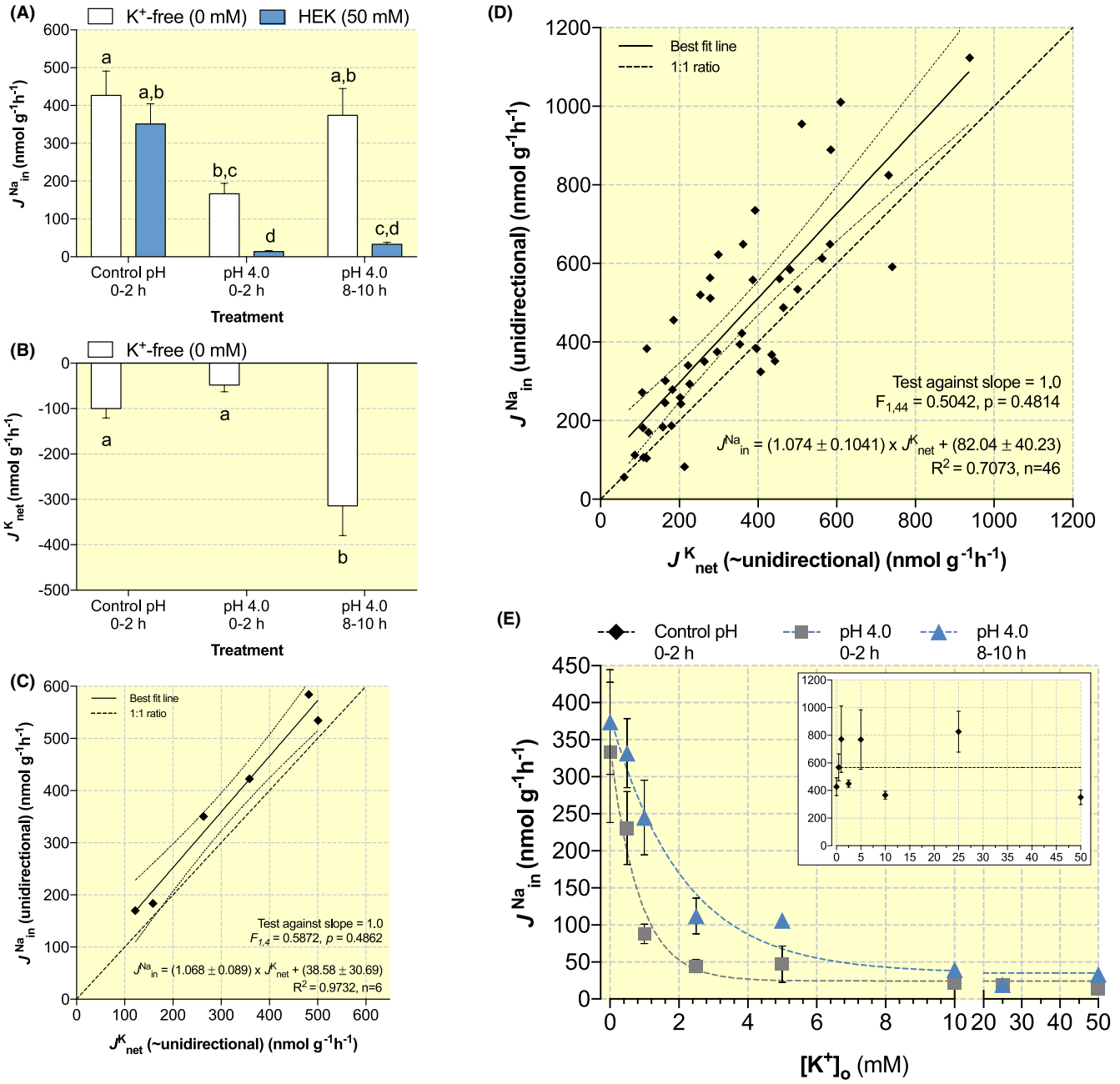

FIGURE 5 The influence of environmental [K$^+$] on zebrafish J^{Na}_{in} dynamics during acid exposure. (A) J^{Na}_{in} was determined in control pH (pH 8.0) or pH 4.0 conditions acutely (0-2 h) or pH 4.0 conditions following 8-10 h of acid exposure and measurements were carried out in media that were either high in $[K^+]_o$ (HEK, 50 mM K$^+$, blue bars) or lacking $[K^+]_o$ (K$^+$-free, 0 mM K$^+$, replaced with 50 mM NMDG, white bars). (B) net K$^+$ loss (J^{K}_{net}) was also measured in all K$^+$-free treatments from (A). Unidirectional J^{Na}_{in} and J^{K}_{net} observations from zebrafish in prolonged acid exposure (8-10 h) from (C) the K$^+$-free group from the present experimental series and from (D) Series 4 (K$^+$-free zebrafish), Series 5 (all zebrafish) and Series 6 (NMDG- and DMSO- control zebrafish) were regressed and the resulting best fit line tested against a slope of 1 (test details in figure). (E) unidirectional J^{Na}_{in} was measured in water with increasing concentrations of $[K^+]_o$ in zebrafish during control pH exposure (inset; black diamonds), acute acid exposure (pH 4.0:0-2 h) exposures; grey squares) or during prolonged acidic conditions (pH 4.0:8-10 h exposure; blue triangles). Data are presented as mean + SE. Data not sharing letters denote significant differences [(A) two-way ANOVA or (B) one-way ANOVA, Tukey's post hoc test making all comparisons (n = 6; $P < .05$)]. In (C, D) the dashed line represents y = x, and the solid line represents line of best fit (95% CI shown as paired dotted lines) with an equation of J^{Na}_{in} (nmol g^{-1} h^{-1}) = (1.068 ± 0.089) × J^{K}_{net} + (38.58 ± 30.69), $R^2 = 0.9732$, $df = 4$ in (C) and J^{Na}_{in} (nmol g^{-1} h^{-1}) = (1.072 ± 0.106) × J^{K}_{net} + (84.81 ± 41.13), $R^2 = 0.7073$, $df = 43$ in (D); the resulting best fit lines were tested against a slope of 1 (test details in figure). In (E) the dotted line represents the line of best fit as predicted by a linear model with a slope not significantly different from 0 (inset; $R^2 = 0.0132$; $F_{1,40} = 1.116$, $P = .2972$) and an intercept of 634.1 ± 73.37 nmol Na$^+$ g^{-1} h^{-1} or a single-phase exponential decay model (0-2 h: J^{Na}_{in} (nmol g^{-1} h^{-1}) = (342.9-24.38 nmol g^{-1} h^{-1}) × ($e^{(-1.204 \times [K+]o\ mM)}$) + 24.38; 8-10 h: (382.7-35.1 nmol g^{-1} h^{-1}) × $e^{(-0.4723 \times [K+]o\ mM)}$ + 35.1 nmol g^{-1} h^{-1}). A comparison of fits analysis determined that the half-inhibition concentration in prolonged acid exposure ($[K^+]_o$ = 1.468 mmol K$^+$ L^{-1}) was statistically greater ($F_{1,90} = 4.999$; $P = .0278$) than that in the acute acid ($[K^+]_o$ = 0.5757 mmol K$^+$ L^{-1}) exposure

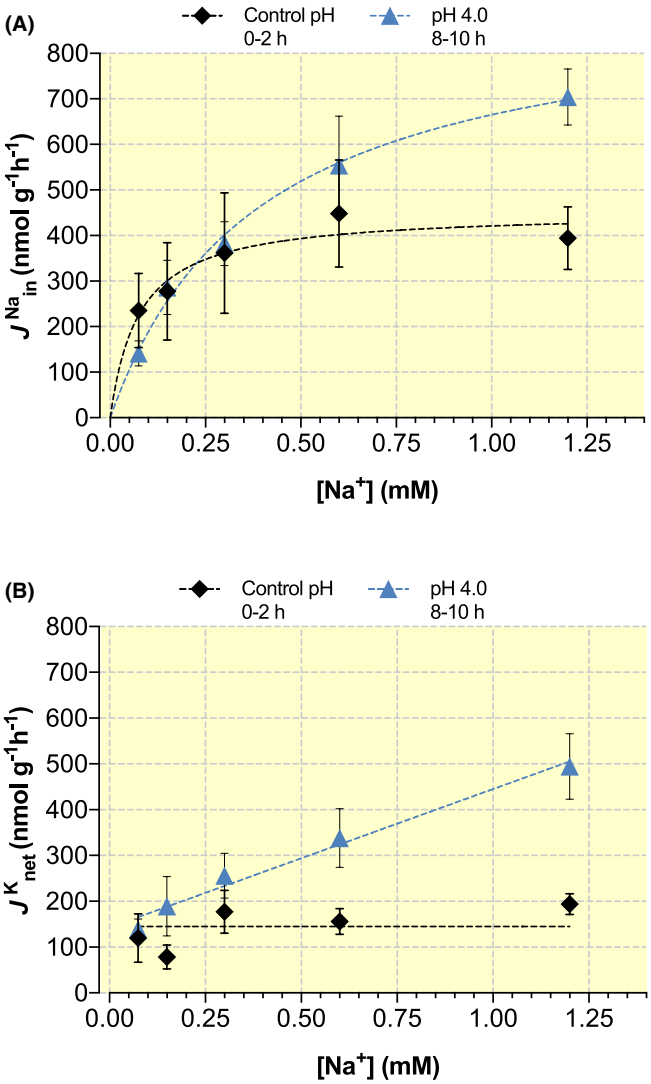

FIGURE 6 Effect of environmental [Na^+] on the transport kinetics of J^{Na}_{in} and J^{K}_{net} during acid exposure. (A) J^{Na}_{in} and (B) J^{K}_{net} were measured in the presence of changing $[Na^+]_o$ (75μM-1.2 mM Na^+) in zebrafish exposed to control pH conditions (pH 8.0; black diamonds) or following 8-10 hours of pre-exposure to acid conditions (pH 4.0:8-10 h; blue triangles). Data are presented as mean + SE. Michaelis-Menten models were fitted to J^{Na}_{in} data, while linear models were fitted to J^{K}_{net} data. J_{max} was calculated to be 453 ± 96.3 nmol g^{-1} h^{-1} in control pH water and 925.8 ± 148.2 nmol g^{-1} h^{-1} at pH 4.0. K_m was calculated to be 75.8 ± 71.7 μM Na^+ in control pH water vs 391.8 ± 151.4 μM Na^+ in pH 4.0 water. In (B), regression analysis on J^{K}_{net} supported a linear model with a slope not significantly different from 0 ($R^2 = 0.1094$; $F_{1,28} = 3.441$, $P = .0742$) with an intercept of 145.1 ± 17.4 nmol K^+ g^{-1} h^{-1} under control pH conditions and a linear $[Na^+]_o$-dependent relationship following 8-10 hours of pre-exposure to acid conditions where J^{K}_{net} (nmol K^+g^{-1} h^{-1}) = 302.2 ± 58.65 × $[Na^+]_o$ mM +143 ± 36.91; $R^2 = 0.4958$ ($F_{1,27} = 26.55$, $P < .0001$)

4-Aminopyridine (4-AP) did not affect J^{Na}_{in} or J^{K}_{net} in any condition (Figure 7B,D). Tetraethylammonium (TEA) also elicited no effects in J^{Na}_{in} or J^{K}_{net} during control pH conditions or for 0-2 hours of pH 4.0 exposure; however, it did significantly impair the restoration of J^{Na}_{in} and concomitant stimulation of J^{K}_{net} for 8-10 hours pH 4.0 exposure (Figure 7C,D).

2.7 | Series 7: mRNA expression of K^+-dependent Na^+/Ca^{2+} exchangers in zebrafish gill

Using RT-PCR and Sanger sequencing, we identified mRNA expression of six genes of the K^+-dependent Na^+/Ca^{2+} exchangers (NCKX;*slc24*) family (*slc24a1, slc24a2, slc24a3, slc24a4a, slc24a5, slc24a6*) in zebrafish gill tissue (Figure 8; primers and amplicon sizes are shown in Table 2).

3 | DISCUSSION

Adult zebrafish exhibited marked reductions in Na^+ uptake at the onset of low pH exposure, which rapidly returned to control rates by 8-10 hours of continued low pH exposure. Our findings suggest that a novel mechanism linked to K^+ excretion is responsible for this re-established J^{Na}_{in} during low pH exposure, which is fundamentally different from well-established Na^+ uptake mechanisms in zebrafish. This novel Na^+ uptake mechanism seems to be electroneutral, relies on outwardly directed 1:1 K^+ efflux, is sensitive to TEA but not to inhibitors of the ion-transporters involved in the reputed mechanisms, and is fundamentally different from the mechanism that is operational under control pH conditions. Since mammalian NCKXs (K^+-dependent Na^+/Ca^{2+} exchangers) match the kinetics and pharmacology observed in zebrafish exposed to low pH, and zebrafish gills express mRNA for six *nckx* isoforms, these K^+-dependent Na^+/Ca^+ exchangers are primary candidates that could mediate the Na^+ uptake mechanism described herein.

As expected, zebrafish exhibited an abrupt impairment (~60%-75% decrease) in J^{Na}_{in} in response to acute (2 hours) acid (pH 4.0) exposure (from ~540 nmol g^{-1} $hour^{-1}$ to ~130 nmol g^{-1} $hour^{-1}$; Figure 2A), suggesting inhibition of the NHE-dominant Na^+ uptake mechanism used during control conditions. We interpret the remaining J^{Na}_{in} that persisted for 0-2 hours of acid exposure (~130 nmol g^{-1} $hour^{-1}$) as non-NHE mediated. It is important to note the ~10 000-fold difference in $[H^+]_o$ that exists between control- and acid-exposure conditions, and its direct impact on J^{Na}_{in} via an NHE. However, during the ensuing time series at pH 4.0, we found that J^{Na}_{in} gradually recovered, returning to control rates within ~8-10 hours. To our knowledge, no other time series data with adult zebrafish during acute

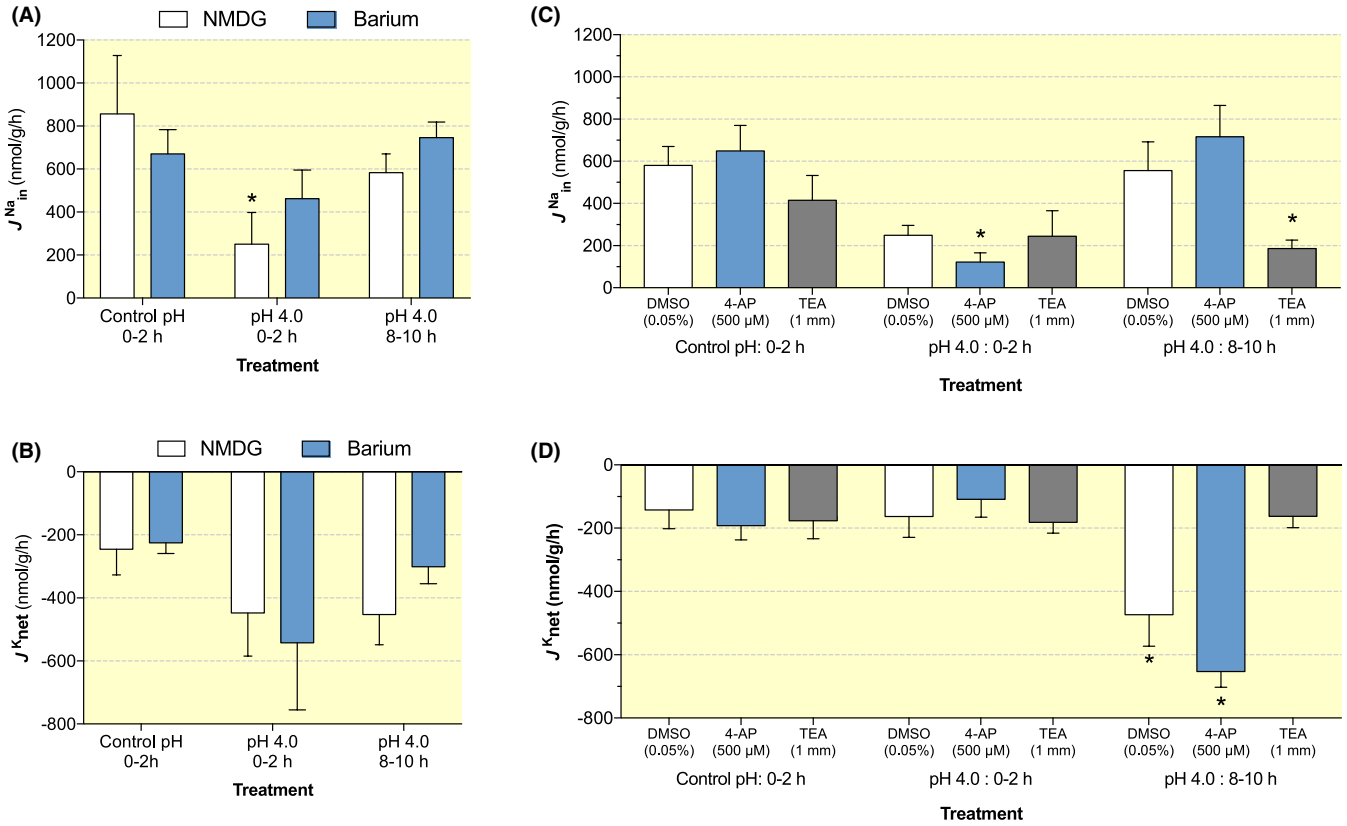

FIGURE 7 Effect of putative K^+ transport inhibitors on unidirectional J^{Na}_{in} uptake and J^{K}_{net} in zebrafish during acid exposure. J^{Na}_{in} (A, C) and J^{K}_{net} (B and D) were determined in control pH (pH 8.0) water or during acute (0-2 h) or prolonged (8-10 h) exposure to pH 4.0 water. Prior to flux measurement, zebrafish were incubated in flux media at indicated pH levels containing either (A, B) Ba^{2+} (10 mM; blue bars) or (C, D) 4-AP (500 μM; blue bars) or TEA (1 mM; grey bars). Vehicle control fluxes were carried out in either (A, B) NMDG (10 MM; black bars) or (C, D) DMSO (0.05%; white bars). Data are presented as mean ± SE. Data presented with asterisks (*) denote significant differences from Vehicle control fluxes (two-way ANOVA; Dunnett's post hoc test against (A, B) NMDG or (C, D) DMSO groups measured in control pH water at 0-2 hr; n = 6, P < .05)

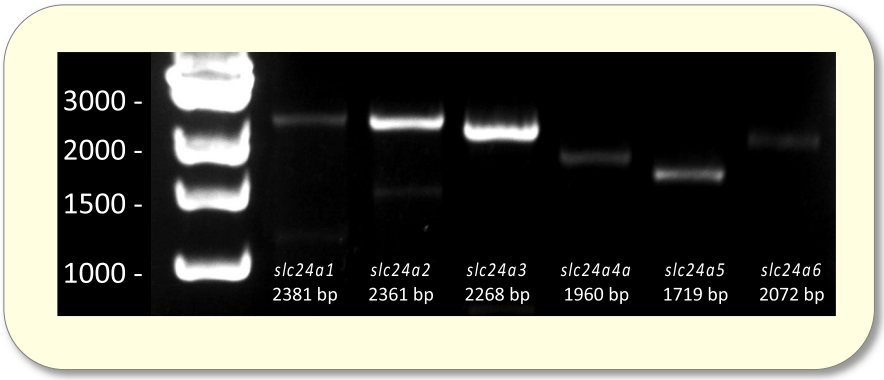

FIGURE 8 mRNA expression of *nckx* isoforms in the gills of adult zebrafish. RT-PCR (35 cycles; Phusion polymerase; New England Biolabs) was conducted on cDNA synthesized from total RNA extracted from gills of control pH (pH 8.0) exposed zebrafish with primers (Table 2) targeting specific isoforms of the slc24 gene family. Amplified products were analysed alongside 1 kb ladder (New England Biolabs)

(<12 hours) acid exposure have been reported; the closest relevant measurement appears to be 3 days post-onset of acid exposure.[59] These studies reported that adult zebrafish exposed to pH 3.8-4.0 for 3 days had similar rates of Na^+ uptake (measured at low pH) compared to rates in control zebrafish (measured at circumneutral pH). After 5 days of acid exposure, the kinetic profile of Na^+ uptake with respect to environmental [Na^+] nearly doubled in J_{max} while affinity for Na^+ decreased sixfold (ie K_m increased).[59] Notably, within 10 hours of acid exposure,

TABLE 2 Transcript-specific primers used for RT-PCR

Transcript	Accession number	Primer sequence (5′-3′)	Annealing temperature, °C	Amplicon (bp)
slc24a1	XM_021473276.1	F: CAT ACC CCT GCA TCT TTT AGC G R: ACC TGT GAA AGA ACT GTG ATG TC	61	2411
slc24a2	XM_017355745.2	F: CCG TAA GTC TGT GGG ATT CTT R: TGG ATG TCC TTG CCT CAT TAA A	61	2361
slc24a3	XM_680210.8	F: GAA CTG GCA CCA AAC TGA CG R: GAA GGA GAG CCT TTC TGC GT	61	2268
slc24a4a	XM_009293194.3	F: CCG ATC CCG AGC CTG ATT TT R: TGG TTC AAA GCC CAT GGA GAA	61	1960
slc24a5	NM_001030280.1	F: TGT GTG TGT TCT CCG TCA TC R: CGC ACT TTG ACT TCT CTT GTA TTT	62	1719
slc24a6	XM_021474309.1	F: TGG AAA GGG CAC ATA TCG GTA A R: AAT AAG GCA GTG ACT GGG GG	64	2153

we too observed a doubling of J_{max} and roughly a fivefold increase in K_m (Figure 6A; discussed below). Whether the underlying mechanisms responsible for re-established Na^+ uptake in the current study (within 10 hours) are the same as those at play following 3- and 5-day exposure times remains to be investigated.

3.1 | The case against NHE or the NHE/Rh metabolon

The recovery of Na^+ influx to control rates during continued acid exposure was insensitive to both amiloride (inhibitor of NHEs, Na^+ channels, and ASICs[34,60]) and EIPA (NHE inhibitor[34]) (Figure 3A). Rescue of NHE function by an Rh-metabolon during acid exposure would involve sustained elevations in $J^{amm}{}_{net}$; however, we only observed a transient increase in $J^{amm}{}_{net}$ that was limited to the earliest time point (0-1 hour) (Figure 2B). The transient rise in $J^{amm}{}_{net}$ may be explained by immediate exposure to low pH creating an acidic $NH_4{}^+$-sink (acid-trapping) for metabolically derived NH_3, suddenly stripping the organism of NH_3 before returning to control flux rates fuelled by metabolism.[61] Overall, the inhibitor results, lack of a persistent increase in $J^{amm}{}_{net}$, throughout exposure and thermodynamic challenges previously described effectively eliminate a role for NHEs – alone or as part of an Rh-mediated metabolon – in the re-established Na^+ uptake during acid exposure. In fact, given the thermodynamic constraints for NHE, we might predict a down-regulation of apical NHE expression within the gill ionocytes so as to prevent a reversal of Na^+/H^+ exchange that would further exacerbate Na^+ loss.

3.2 | The case against Na^+ channels/ASICs

Na^+ movement through Na^+ channels/ASICs is electrogenically tied to VHA-mediated H^+ excretion, and carbonic anhydrase (CA) activity is predicted to provide H^+ as substrate for VHA. Thus, a Na^+ channel/ASIC mechanism would entail an increase in net acid efflux. However, we noted no overall effects of time or treatment in either J^{TA-HCO_3-} (Figure 2C) or $J^{H}{}_{net}$ (Figure 2D). Taken together with the lack of sensitivity to DAPI (Figure 3A; ASIC inhibitor[36]), phenamil (Figure 3B; Na^+ channel inhibitor[39]) and acetazolamide (Figure 3C; CA inhibitor[10,47]) during either acute (0-2 hours) or prolonged (8-10 hours) acid exposure, these results indicate that the re-established $J^{Na}{}_{in}$ during acid exposure was not mediated via ASIC or Na^+ channels.

While insensitivity to phenamil was expected given the lack of an identifiable ENaC orthologue in zebrafish genome databases[62] (also undetected within current GRCz11 assembly, GCA_000002035.4), insensitivity to DAPI during control conditions was surprising given that zebrafish gills express mRNA for all six zebrafish ASIC isoforms over a wide range of environmental [Na^+] (~50 to 1300 μM).[9] Furthermore, Dymowska et al[9] reported that roughly 50% of Na^+ uptake in adult zebrafish acclimated to low environmental ion levels and control pH ([Na^+]: ~500 μM, [Cl^-]: ~300 μM, [Ca^{2+}]: ~1.2 mM, pH ~8.5) was sensitive to DAPI (10 μM) and amiloride (200 μM), but not EIPA (100 μM).[9] However, in that same study, zebrafish exposed to ultra-low environmental ion levels and slightly acidic pH ([Na^+]: ~50 μM, [Cl^-]: ~60 μM, [Ca^{2+}]: ~300 μM, pH ~6) exhibited no sensitivity whatsoever to either DAPI or EIPA. Both the ultra-low water chemistry

used by Dymowska et al[9] and the low pH conditions in the present study would present adverse gradients for the function of an NHE for Na^+ uptake. Since both studies reported a similar lack of pharmacological blockade with either amiloride, EIPA, DAPI or phenamil, the putative H^+-linked Na^+ uptake models do not seem to be functional under these conditions. A possible explanation may be that ASICs can function only when fish are exposed to moderately low $[Na^+]_o$ and pH but not in either ultra-low $[Na^+]_o$ or very low pH.

3.3 | The case against NCC

To evaluate the putative role for NCC in the recovery of J^{Na}_{in} during acid exposure, we tested a possible link to environmental Cl^-. One flux experiment utilized Cl^--free media to evaluate the role of NCC following transfer from acid exposure to control pH conditions (ie recovery from an acid exposure), while a separate flux experiment evaluated the role of NCC during the acid exposure. While Kwong and Perry[13] noted stimulations in J^{Na}_{in} following transfer to control pH conditions in larval zebrafish, we observed no such effect in our adult zebrafish (Figure 4A), perhaps indicating life stage-specific differences. In addition, removal of environmental Cl^- did not affect the ability of our adult zebrafish to recover J^{Na}_{in} following low pH-exposure at any time-point, nor did it inhibit the residual pH-independent J^{Na}_{in} observed during acute low pH exposure (Figure 4B). Furthermore, applications of HCT and metolazone (NCC inhibitors[37,43–46]), or bumetanide (an inhibitor of both NCCs and NKCCs[37,42]), also had no effects on Na^+ uptake in any flux treatment (Figure 3B,C). Most importantly, the recovery of J^{Na}_{in} at 8-10 hours of continued acid exposure was not attenuated in Cl^--free conditions. From these results, combined with the thermodynamic challenges raised in the Introduction, we can conclude that NCC is not a relevant mechanism explaining the return of Na^+ uptake during acid exposure.

3.4 | The case for a K^+-dependent Na^+ uptake mechanism

After systematically ruling out roles of each of the three putative Na^+ uptake mechanisms in the re-established J^{Na}_{in} during acid exposure, we re-visited first principles of ion exchange in relation to water chemistry to assess what other possible driving gradients could be used to re-establish J^{Na}_{in} in low pH conditions. While environmental $[K^+]_o$ in our experiments was extremely low (~4 μM), K^+ is the primary inorganic ion in the intracellular pool[63] with an estimated average intracellular $[K^+]$ ($[K^+]_i$) in teleost gill ranging from ~14-90 mM.[64,65] Furthermore, Na^+-K-ATPase activity in ionocytes is bound to result in $[K^+]_i$ in the upper range (or perhaps higher) along with very low $[Na^+]_i$ in these cells. The resulting diffusion gradient (4 μM $[K^+]_o$ vs 14 000-90 000 μM $[K^+]_i$) could provide a very large, outwardly directed ion-motive force. And while K^+ extrusion in exchange for Na^+ uptake has been traditionally argued against because of the low K^+ permeability of goldfish (*Carassius auratus*) gills,[66] to our knowledge there are no studies examining K^+ efflux rate in conjunction with unidirectional Na^+ uptake during low pH exposure. That said, a limited number of studies examining net Na^+ and K^+ efflux in several species of Amazonian fishes have reported stimulations in J^{K}_{net} either within 1 hour of low pH exposure (pH ≤3.5)[67] or following gradual decrements in water pH.[68] Intriguingly, in the latter study, stimulations of J^{K}_{net} loss following 18 hours of low pH (pH 4.0) exposure were associated with reductions in J^{Na}_{net} loss, compared to measurements at 1 hour of exposure in all three fish species studies [tamoatá (*Hoplosternum littorale*), matrincha (*Brycon erythopterum*) and tambaqui (*Colossoma macropomum*)]; however unidirectional Na^+ fluxes would be needed to correctly compare these results to our own.

If we apply the intracellular $[K^+]_i$ and environmental $[K^+]_o$ to models of electroneutral counter-transport,[20] we find that K^+ efflux could clearly drive electroneutral Na^+/K^+ exchange. Therefore, we tested whether K^+ efflux was responsible for re-establishing Na^+ uptake during low pH exposure by measuring J^{Na}_{in} in HEK (50 mM K^+). By eliminating (or perhaps reversing) K^+ efflux, HEK would be predicted to inhibit K^+-dependent Na^+ uptake but only during acid exposure (Figure 5A). Indeed, HEK had no effect on J^{Na}_{in} during control pH exposure, which matched the observed low K^+ permeability in goldfish gills,[66] but remarkably, HEK induced a near-complete abolishment of J^{Na}_{in} during both short-term (0-2 hours) and continued (8-10 hours) acid exposure. Thus, disruption of the outwardly directed K^+ gradient effectively abolished the NHE-independent mediated J^{Na}_{in} that persisted during low pH exposure. These results support a K^+-efflux-driven Na^+ uptake mechanism that gets activated and progressively gains importance during exposure to low environmental pH.

For completeness, we also tested the effect of K^+-free water on J^{Na}_{in} but found no effects during control conditions, during short-term (0-2 hours) acid exposure to low pH (ie zebrafish experienced the typical ~60% reduction in J^{Na}_{in}) or during continued (8-10 hours) acid exposure (ie zebrafish fully recovered J^{Na}_{in}) (Figure 5A).

We next examined the net K^+ loss (J^{K}_{net}) during acid exposure. In zebrafish exposed to K^+-free conditions, J^{K}_{net} was negative (ie a small net loss from the animal) with

similar rates during control pH conditions and during acute (0-2 hours) pH 4.0 exposure (Figure 5B). However, zebrafish continuously exposed to pH 4.0 for 8-10 hours experienced an approximately fourfold increase in outwardly directed J^{K}_{net}. This increase, paired with the strong 1:1 relationship between K^+ loss and Na^+ uptake rates observed in Series 4 (Figure 5C) and further supported by regression of all 8-10 hours J^{K}_{net} and J^{Na}_{in} data collected from Series 4 (K^+-free zebrafish), Series 5 (all zebrafish) and Series 6 (NMDG- and DMSO- control zebrafish) (Figure 5D) indicated a functional relationship between the two, but only during low pH conditions.

Importantly, J^{Na}_{in} was independent from environmental $[K^+]_o$ during control conditions but was strongly inhibited by increasing $[K]_o$ during both acute and sustained acid exposure (Figure 5E), supporting the idea that K^+ efflux plays a critical role in re-establishing Na^+ uptake during acid exposure. Furthermore, our kinetic analysis revealed that the half-life constant (interpreted as a proxy to K_i; the exposure concentration of K^+ that causes 50% inhibition of J^{Na}_{in}) was significantly greater following prolonged acid exposure compared to acute acid exposure. Thus, the potency of environmental $[K^+]_o$ as a competitive inhibitor diminished following 8-10 hours of exposure, suggesting a progressive upregulation of the mechanism responsible for the increased J^{Na}_{in}. Put another way, during continued acid exposure, zebrafish are progressively upregulating an Na^+/K^+ exchange mechanism which in effect elicits a higher internal affinity for K^+.

We also found that prolonged acid exposure caused dramatic shifts in the $[Na^+]_o$-dependent kinetics of both J^{Na}_{in} and J^{K}_{net}. With regards to J^{Na}_{in} we found that J_{max} roughly doubled in response to 8-10 hours of acid exposure, while the K_m was approximately fivefold greater (Figure 6A). Thus, maximum Na^+ transport capacity doubled, whereas Na^+ transport affinity decreased by fivefold after 8-10 hours exposure to pH 4.0. In examining J^{K}_{net} patterns in the same experimental series, J^{K}_{net} was determined to be independent of $[Na^+]_o$ during control pH conditions, while 8-10 hours of acid exposure induced a J^{K}_{net} pattern that was strongly dependent upon $[Na^+]_o$ suggesting a clear linkage between K^+ efflux and Na^+ uptake in longer-term acid-exposed zebrafish (Figure 6B). Taken together, these data indicate the upregulation of a novel Na^+ uptake mechanism during acid exposure with markedly different kinetics, substrates and ion-motive forces compared to the NHE-dependent mechanism utilized during control conditions.

In vertebrates, K^+ is a major intracellular monovalent cation and is maintained at >20-fold higher than extracellular K^+ levels[69] and up to ~22 500-fold higher than $[K^+]_o$ observed in the current study. K^+ is generally available via the diet in excess of requirements.[70] Plasma $[K^+]$ for freshwater fishes ranges from 4 to 5 mM[71] while average intracellular $[K^+]$ throughout the body ranges 80-90 mM. Assuming a blood volume of ~4% and a ~66% intracellular volume in a 500-mg zebrafish, the total estimated on-board K^+ would be ~30 000 nmols K^+, which could sustain the upregulated K^+-dependent J^{Na}_{in} operating at ~400 nmol g^{-1} $hour^{-1}$ for ~15 hours before experiencing a 10% reduction in whole-body K^+ (hypokalaemia). These calculations illustrate that a putative Na^+/K^+ exchange mechanism could sustainably operate during acid exposure indefinitely, so long as the animal can replenish K^+ stores by feeding.

3.5 | Evaluating potential K^+ transport pathways

K^+ is transported across membranes via a variety of transport proteins including NKA, H^+-K^+-ATPase (HKA), NKCC, and NCKXs. For NKA to play a direct role, the transporter would need to be operating on the apical surface of gill ionocytes and in the reverse direction. To our knowledge, there are no reports about apical NKA in gill cells, operating in either direction. Similarly, HKA takes up, rather than excretes, K^+; in any case, the current zebrafish GRCz11 genome assembly does not possess HKA homologues. Furthermore, a mechanism involving HKA would rely on the concomitant involvement of a Na^+ channel as well as CA, for which we found no evidence (Figure 3A-C). A lack of inhibition by bumetanide on the restored J^{Na}_{in} (Figure 3B) rules out NKCC as well. K^+ channels are subcategorized into Ca^{2+}-activated, tandem pore domain, inward rectifying, and voltage-gated K^+ channels. Recent studies have implicated the apical inwardly rectifying K^+ channel, ROMK (also known as kcnj1 or kir1.1) in K^+ secretion in freshwater gill ionocytes. However, if K^+ channels were indeed playing a role, it would again likely involve linkage to a Na^+ channel mechanism.

Ba^{2+} is a broad K^+ channel inhibitor that targets Ca^{2+}-activated K^+ channels, tandem pore K^+ channels, along with ROMK and other inwardly rectifying K^+ currents.[16,48–50,72,73] We observed no inhibitory effect of Ba^{2+} on J^{Na}_{in} or J^{K}_{net} during control pH conditions or during either acute or prolonged acid exposure in relation to measurements in NMDG-exposed zebrafish during control pH exposure. 4-AP (inhibitor of voltage-gated K^+ channels[74]) did not elicit any deviations from the typical J^{Na}_{in} inhibition and recovery patterns in any of the treatments (Figure 7C,D). TEA (a non-specific inhibitor of Ca^{2+}-activated K^+ channels,[53,54] voltage-gated K^+ channels,[55] NKA[56] and NCKXs[57,58]) also elicited no effects on either J^{Na}_{in} or outward J^{K}_{net} during either control pH or acute pH 4.0 conditions. Intriguingly, TEA did inhibit

both the restoration of J^{Na}_{in} and concomitant increase in outward J^{K}_{net} in zebrafish during prolonged acid exposure. Since the Ba^{2+} and 4-AP results had ruled out roles for Ca^{2+}-activated K^+ channels or Kv1 channels, and the lack of effect of TEA on J^{Na}_{in} during control pH exposure rules out NKA, we are left with the possibilities that either NKCXs play a role in the K^+-dependent J^{Na}_{in} mechanism that is activated upon acid exposure, or that we have discovered a completely new mechanism.

NCKXs are a family of low-affinity/high capacity ion transporters which exchange inward-moving Na^+ for outward-moving K^+ and Ca^{2+}.[75] Mammals possess five NCKX genes (NCKX1-5) that are often regarded as Ca^{2+} transporters with putative roles in sperm flagellar beating,[76] retinal cone phototransduction,[77] skin pigmentation[78] and neuronal function.[79] In addition, NCKXs are expressed in vascular smooth muscle, thymus, lungs, epidermal cells, intestine and kidney[80–83]; however, their roles in transepithelial Na^+ transport has never before been considered. Zebrafish possess seven *nckx* genes within their annotated genome; of these, we were able to detect mRNA expression of six (*slc24a1, slc24a2, slc24a3, slc24a4a, slc24a5, slc24a6*) within gill tissue through RT-PCR (Figure 8). The proposed stoichiometry of NKCX1 and NCKX2 has been determined experimentally as $4Na^+/1Ca^{2+}+1K^+$[84]; however, these relationships have yet to be elucidated for other isoforms and in other species. Given that the NCKX family mediates K^+-dependent Na^+ transport, these transporters currently are the most likely molecular candidates to consider for the observed re-established Na^+ uptake.

3.6 | Summary and significance

During control conditions, J^{Na}_{in} uptake in adult zebrafish primarily occurs via well-characterized NHE-dependent mechanisms. However, when zebrafish are exposed to low pH water, NHE function is thermodynamically inhibited, yet J^{Na}_{in} is gradually restored back to control rates over time. Pharmacological inhibitor experiments using concentrations known to be effective in previous studies in teleosts (Table 1) failed to attribute this restored Na^+ uptake to reputed models.

To overcome the limitations often cited in inhibitor-based studies, we made use of alternative approaches to further evaluate potential contributions from established models in the restored J^{Na}_{in} namely, the NHE-Rh metabolon model was evaluated by measuring J^{amm}_{net} and J^{H}_{net} measurements; the VHA-linked ASIC/Na^+ channel was evaluated by measuring J^{H}_{net} and the NCC model was evaluated by measuring J^{Na}_{in} in Cl^--free media.

Thus, by considering our inhibitor data alongside these alternative approaches, we were able to rule out the involvement of existing Na^+ uptake models in fish. Instead, through consideration of first principles of ion-exchange, we identified and functionally characterized a novel Na^+ uptake mechanism that relies on the equimolar efflux of K^+ in adult zebrafish. The presence of six *nckx* isoforms in zebrafish gills combined with the observed sensitivity of the K^+-dependent Na^+ uptake to TEA inhibition points to NCKXs as likely molecular candidates mediating this novel mechanism; however, this will need to be confirmed through future molecular, cell biology, kinetics, and histochemical experiments.

It is important to note that the zebrafish has now become a model system for understanding ion transport at low pH[9,13,19,28–30,32,33,59] as discussed in detail by Kwong et al.[85] We now know that many other teleosts of the Order Cypriniformes (to which zebrafish belong), as well as the Orders Perciformes, Characiformes, Siluriformes and Cichliformes, also inhabit waters at pH 4.0 and below, yet still maintain Na^+ homeostasis.[85–87] Given the wide geographic distributions and phylogenetic relationships in these teleost species, it would be intriguing to determine if the ability to invoke similar K^+-dependent Na^+ uptake mechanisms allow these fishes to inhabit low pH environments, providing a competitive advantage and thus allowing for their expansion to their realized niches. Our findings thus provide an impetus to look for similar functions in fish inhabiting or transiting low pH environments such as Amazonian water bodies and acid rain contaminated lakes.[86,87]

In summary, the functional identification of this novel Na^+ uptake pathway opens a new avenue within the study of Na^+ uptake in freshwater fishes and more broadly the fields of ion and acid-base regulation and comparative physiology. Future elucidation of the molecular mechanism responsible for Na^+/K^+ exchange is a crucial next step, as is understanding how the mechanism is regulated, and specifically identifying its cellular location. Zebrafish have at least five different types of gill ionocytes.[88] Does this new mechanism reside within one or more types of these characterized ionocytes, or are there other subtypes that are yet to be identified? Are there other environmental challenges where this mechanism plays a role for teleosts? Is there some inherent cost of K^+-dependent Na^+ uptake which makes it only worth employing during low pH exposure? These and many other questions regarding this novel K^+-dependent Na^+ uptake mechanism await investigation.

4 | MATERIALS AND METHODS

4.1 | Experimental animals and holding

Zebrafish (*Danio rerio*; 150-500 mg; total N = 701) were obtained from a local pet store and were kept in two

50-L aerated glass aquaria (up to 200 fish per tank), with a 14:10 hours light/dark photoperiod at room temperature (20-22°C). Upon acquisition, fish were acclimated for at least 2 weeks to holding conditions (Na^+: 1.1 mM, Ca^{2+}: 2.1 mM, Cl^-: 4.1 mM, Mg^{2+}: 6.5 μM, K^+: 3.84 μM, SO_4^{2-}: 10.41 μM, pH ~8.0) prior to any experimentation. Tanks were supplied with gentle aeration and were fitted with a biological filter. Water was refreshed bi-weekly with a 50% water change with prepared holding water. Fish were fed commercial fish food (Tetramin® tropical flakes, Tetra Spectrum Brands Pet LLC), *ad libitum* over 30 minutes, three times a week, with food being withheld for 48 hours prior to experimentation. Fish were transferred from general holding to exposure aquaria (15-L aquaria with aeration) to settle overnight prior to experimentation. All zebrafish were used under the University of British Columbia Animal Care Protocol A14-0251.

4.2 | Reagents

Unless noted otherwise, all chemical compounds, reagents and enzymes were supplied by Sigma–Aldrich Chemical Company. Ethyl 3-aminobenzoate methanesulfonate (MS222) was obtained from Syndel laboratories (Nanaimo, BC, Canada). Radio-labelled ^{22}Na (as $^{22}NaCl$) was purchased from Perkin Elmer, activity = 1 μCi μL^{-1}). All reagents and buffers were prepared in deionized water and all pharmacological agents were dissolved in 0.05% DMSO, unless otherwise specified. Vehicle control experiments with 0.05% DMSO alone were also performed.

4.3 | Experimental protocols

4.3.1 | Series 1: Time-course dynamics of zebrafish ion-regulatory status during acid exposure

Preliminary rangefinder experiments indicated that acute (2-hour) pH 4.0 exposure elicited a ~65% inhibition in J^{Na}_{in} compared to rates observed in control pH exposed zebrafish, while animals exposed to pH 3.5 exhibited a ~90% inhibition. While no deaths were observed at either of the low pH exposures, towards the end of the 2 hour pH 3.5 exposure, zebrafish appeared inactive and listless; thus, we elected to utilize pH 4.0 as an exposure pH for the remainder of our experiments.

Zebrafish (n = 42 per group) were exposed to either control (pH 8.0 ± 0.1) or acidic (pH 4.0 ± 0.05) water for up to 12 hours. To maintain acidic conditions during exposure, a Radiometer (Radiometer-Copenhagen, Brønshøj, Denmark) pH-stat system consisting of a pH meter (PHM82), combination glass-bodied pH electrode (GK24O1C) and an auto-titration controller (TTT-80) metered the addition of acid titrant (0.1 M HCl) via a solenoid valve into the experimental chamber. At marked times (0, 1, 2, 4, 6, 8 and 10 hours) during the 12-hour exposure period, subsets of individual zebrafish (n = 6) from each treatment were transferred from exposure aquaria into individual 50-mL flux chambers (one fish per flux chamber) containing known volumes of pH-matched media (ie either pH 8.0 or 4.0) spiked with ^{22}Na (0.02 μCi mL^{-1}); aeration was provided to promote mixing. Rates of unidirectional Na^+ uptake (J^{Na}_{in}) were determined using standard radiotracer methods, measuring the appearance of ^{22}Na in the fish over a 1-2 hours period. During flux experiments, water samples (15-mL) were removed both immediately following the addition of fish and at the conclusion of the flux period for later determination of ^{22}Na gamma radioactivity, total [Na^+], total ammonia ([NH_4^+] + [NH_3]) and titratable acidity minus bicarbonate (TA-HCO_3^-). Following final water sample collection, zebrafish were quickly washed in a high salt bath (200 mM NaCl of appropriate pH) for 1 minute to rinse residual radioactivity from the cutaneous surface, then euthanized via overdose of MS222 (1 g L^{-1} MS222 buffered with 2 g L^{-1} $NaHCO_3$) then individually weighed and analysed for ^{22}Na gamma radioactivity.

4.3.2 | Series 2: Pharmacological profile of the re-established Na^+ uptake mechanism during acid exposure

Zebrafish (n = 6 per treatment) were transferred directly from acclimation/exposure conditions to flux chambers containing media spiked with DMSO (0.05%; vehicle control) or one of several pharmacological inhibitors targeting various Na^+ and other related acid/base transport mechanisms (See Table 1 for inhibitors, putative targets, exposure concentrations and references to previous studies substantiating these concentrations). Zebrafish held in non-acidic conditions were transferred to individual chambers held at either control (8.0) or acidic (4.0) pH levels, while zebrafish exposed to pH 4.0 for 8 hours (as above) were transferred to individual chambers held continuously at acidic pH 4.0. For these flux protocols, zebrafish were allowed to incubate in inhibitor-spiked flux media for 30 minutes to allow time for the blocker to take effect. Flux chambers were then inoculated with ^{22}Na (0.02 μCi mL^{-1}), gently pipette-mixed, then after 5 minutes, sampled for water (15 mL) to initiate the beginning of a 1.5-hours flux period. Flux protocols otherwise matched those that were adhered to in Series 1 experiments.

4.3.3 | Series 3: Investigating the role of [Cl^-] in the re-establishment of J^{Na}_{in} during and after acid exposure

To test for the influence of environmental [Cl^-] on Na^+ uptake, zebrafish were exposed to either control or acidic conditions for up to 8 hours (as above). Following either 0 hour (no-exposure control), 2, or 8 hours of acid exposure, a subset of zebrafish (n = 6 per treatment) was transferred into individual flux chambers filled with either Cl^--containing media (2.032 mM $CaCl_2$; 1.1 mM $NaHCO_3$; 6.5 μM $MgSO_4$; 3.91 μM CaSO4; 3.84 μM KCl) or Cl^--free media (2.036 mM $CaSO_4$; 1.1 mM $NaHCO_3$; 6.5 μM $MgSO_4$; 1.92 μM K_2SO_4), both of which were set to control pH and spiked with ^{22}Na (0.02 μCi mL^{-1}). A second subset of zebrafish (n = 9 per group) undergoing exposure to control or acidic conditions was similarly transferred to $^{22}Na^+$-spiked media that were either Cl^--containing or Cl^--free, however, in this iteration the flux media was set to either control pH, or pH 4.0 by titration with 0.1 M H_2SO_4, so as to match the pH condition from which the zebrafish had been transferred. Flux protocols (2 hours) were otherwise carried out as in described in Series 1, with water samples (15 mL) measured for total [Na^+] and both water samples and euthanized fish analysed for ^{22}Na gamma radioactivity.

4.3.4 | Series 4: Investigating the role of environmental $[K^+]_o$ in the re-established Na^+ uptake mechanism during acid exposure

Pre-flux exposure conditions and post-transfer flux treatments matched those protocols used in Series 2 (ie fluxes measured at control pH, and at pH 4.0 at 0-2 and at 8-10 hours after transfer to pH 4.0; n = 6 per group). However, in this series of experiments, a subset of zebrafish was transferred into ^{22}Na-spiked (0.02μCi mL^{-1}) flux media modified to be either nominally K^+ -free or high in $[K^+]_o$. The composition of the K^+-free medium was 3.84 μM KCl, 50 mM N-Methyl-D-glucamine (NMDG) 2 mM $CaCl_2$, 1 mM $NaHCO_3$, 6.5 μM $MgSO_4$, 3.91 μM $MgSO_4$, and the high $[K^+]_o$ medium (HEK) was 25 mM K_2SO_4, 3.84 μM KCl, 2 mM $CaCl_2$, 1 mM $NaHCO_3$, 6.5 μM $MgSO_4$, 3.91 μM $MgSO_4$. Both experimental media were first titrated to pH 8.0 with H_2SO_4, and the low pH medium was thereafter titrated to pH 4.0 with HCl. A second subset of zebrafish (n = 6 per group) was transferred to and similarly tested in media containing different $[K^+]_o$ (0.5, 1, 2.5, 5, 10, 25 mM; prepared by mixing aforementioned K^+-free and HEK media in appropriate proportions) set to the above pH conditions. Flux periods (2 hours) were initiated upon removal of the initial water sample (15 mL) and otherwise matched protocols were adhered to in Series 2. In addition to the measurement of total $[Na^+]_o$ and radioactive ^{22}Na, water samples were also measured for $[K^+]_o$ (see *Water analysis* below).

4.3.5 | Series 5: Profiling the influence of environmental Na^+ on the dynamics of J^{Na}_{in} and J^{K}_{net} during acid exposure

In this experimental series, the influence of $[Na^+]_o$ on $J^{Na}{}_{in}$ and $J^{K}{}_{net}$) during control conditions and following 8 hours of acid exposure (pH 4.0:8-10 hours) was investigated by transferring acclimated/exposed zebrafish (n = 6 per group) to ^{22}Na-spiked flux chambers containing different $[Na^+]_o$ (75, 150, 300, 600, 1200 μM) prepared by mixing volumes of Na^+-containing (2 mM Na-HEPES, 2 mM $CaCl_2$, 6.5 μM $MgSO_4$, 3.91 μM $CaSO_4$, 3.84 μM KCl) and Na^+-free [2 mM NMDG (NMDG-SO_4 to pH 8.0 and thereafter NDMG-HCl to pH 4.0, 2 mM $CaCl_2$, 6.5 μM $MgSO_4$, 3.91 μM $CaSO_4$, 3.84 μM KCl)]. Prior to the addition of zebrafish, flux media were spiked with ^{22}Na (ranging from 12.5-20 nCi mL^{-1}) such that the final specific activity with respect to Na^+ content was 16.67-33.33 μCi $mmol^{-1}$ in the bathing solution. Flux protocols and sampling otherwise matched those described in Series 2.

4.3.6 | Series 6: Effect of K^+ transporter inhibition on the re-established Na^+ uptake mechanism during acid exposure

Pre-flux exposure conditions and post-transfer flux treatments matched those protocols used in Series 2. Zebrafish (n = 6 per group) were transferred to flux chambers containing putative inhibitors and chemical antagonists against known K^+ transport pathways (See Table 1). A subset of zebrafish was transferred to either barium-spiked flux media (10 mM $BaCl_2$, 10 mM mannitol, 2 mM $CaCl_2$, 1 mM $NaHCO_3$, 6.5 μM $MgSO_4$, 3.91 μM $CaSO_4$, 3.84 μM KCl) or NMDG-spiked flux media (20 mM NMDG-SO_4, 2 mM $CaCl_2$, 1 mM $NaHCO_3$, 6.5 μM $MgSO_4$, 3.91 μM $CaSO_4$, 3.84 μM KCl) as a control, while a second subset of zebrafish (n = 6 per group) was transferred to media spiked either with DMSO (0.05%) or the pharmaceutical inhibitor dissolved in DMSO). The pH of these flux solutions was set to pH 8.0 with H_2SO_4 and thereafter to pH 4.0 with HCl. Fish were allowed to incubate for 30 minute prior to the addition of ^{22}Na (0.02 μCi mL^{-1}), after which flux protocols (1.5 hours) were carried out as described in Series 2.

4.3.7 | Series 7: mRNA expression of K^+-dependent Na^+/Ca^{2+} exchangers in zebrafish gill

Lab-acclimated zebrafish were euthanized, and gill tissue was excised and snap-frozen in RNA later. Total RNA was isolated from tissue using a commercially available kit (RNeasy® Mini Kit; Qiagen) according to the manufacturer's protocol and quantified using a NanoDrop® ND-1000 UV-vis spectrophotometer (NanoDrop Technologies). First-strand cDNA synthesis was conducted from 1 μg of RNA with random hexamer primers using a commercially available kit (Superscript™ IV First-Strand Synthesis System; Invitrogen) per manufacturer's instructions.

RT-PCR primers targeting zebrafish-specific mRNA transcripts of *nckx* isoforms (slc24a1, slc24a2, slc24a3, slc24a4a, slc24a5, slc24a6) were designed using NCBI-Primer-BLAST (Table 2). Amplification was performed using Phusion polymerase (New England Biolabs) and the following reaction conditions; 98°C for 1 minute of initial denaturation followed by 35 cycles of denaturation at 98°C for 10 seconds, annealing at 61-64°C for 30 seconds (Table 2), and elongation at 72°C for 1 minute 45 seconds, followed by a final elongation at 72°C for 10 minutes. PCR products were visualized by 1% agarose gel electrophoresis followed by SYBR™Safe staining (Invitrogen). Bands of interest were excised and purified; sequence identity of amplified products was confirmed by Sanger sequencing (Retrogen, Inc.).

4.4 | Water analysis

Water samples were analysed for ^{22}Na gamma radioactivity and total $[Na^+]_o$ in all experimental series, and additionally for total [ammonia] ($T_{[Amm]}$), $[K^+]_o$, and titratable acidity minus bicarbonate ($TA - HCO_{3-}$) as indicated above for some of the experimental series. Measurements of ^{22}Na gamma radioactivity were conducted both on individual zebrafish carcasses and on 1-mL aliquots of initial and final experimental water samples on a Perkin Elmer Wallac Wizard 1480 Automatic Gamma Counter (Waltham, MA). Water total $[Na^+]_o$ and $[K^+]_o$ were measured by atomic absorption flame spectrophotometry (Varian Model 1275, Mulgrave). Water $T_{[Amm]}$ and $TA - HCO_{3-}$ were measured as previously described to calculate $J^H{}_{net}$.[89]

4.5 | Calculations

Rates of Na^+ uptake ($J^{Na}{}_{in}$; nmol g^{-1} $hour^{-1}$) were calculated as:

$$J^{Na}{}_{in} = \left((CPM_{fish} \cdot SA) \cdot \frac{1}{m} \cdot \frac{1}{\Delta t}\right) \quad (2)$$

where CPM_{fish} is the measured counts per minute in the fish, m is the animal mass (g), Δt is the duration of the flux period, SA refers to mean specific activity (nmol CPM^{-1}), which was calculated as:

$$SA = \frac{\left(\frac{[Na^+]_i}{CPM_i} + \frac{[Na^+]_f}{CPM_f}\right)}{2} \quad (3)$$

where $[Na^+]_i$, $[Na^+]_f$ CPM_i and CPM_f correspond to the $[Na^+]_o$ and CPMs of initial and final collected water samples. Net flux rates of total ammonia ($J^{amm}{}_{net}$), were calculated as:

$$J^{amm}{}_{net} = \left([Amm]_f - [Amm]_i\right) \cdot \frac{1}{m} \cdot \frac{1}{\Delta t} \quad (4)$$

where $[Amm]_i$ and $[Amm]_f$ refer to the total ammonia concentration in initial and final water samples, V refers to the flux volume and other notations correspond as above. Analogous equations were utilized to calculate net K^+ flux ($J^K{}_{net}$).

4.6 | Statistical analyses

All data are presented as mean ± SE. A fiducial limit of $P < .05$ was set for all statistical comparisons with all statistical and regression analyses conducted using Prism 7 for Mac (Graphpad). All data were assessed to meet the assumptions of normality and homoscedasticity prior to being analysd using either one-way or two-way analysis of variance (ANOVA). Data not meeting the aforementioned assumptions were rank-transformed and reassessed against the assumptions of ANOVA and rank-transformed data were thereafter utilized in ANOVA assessment and subsequent *post hoc* analysis. Non-parametric analysis was utilized when assumptions were unable to be met, with Dunnett's test applied for multiple comparisons against a control group. Differences amongst groups were determined via Tukey or Sidak *post hoc* tests where appropriate. In Series 4, correlations between $J^K{}_{net}$ and $J^{Na}{}_{in}$ measured in K^+-free conditions, and between $J^{Na}{}_{in}$ and $[K^+]_o$ measured during control pH exposure were evaluated using Pearson's correlation coefficient and linear regression analysis. In these regression analyses, the slope of the line of best fit was tested against the null hypothesis of slope = 1 ($J^K{}_{net}$ versus $J^{Na}{}_{in}$) or slope = 0 ($[K^+]_o$ versus $J^{Na}{}_{in}$). Correlations between $J^{Na}{}_{in}$ and $[K^+]_o$ measured

during either acute (0-2 hours) or prolonged (8-10 hours) pH 4.0 exposure in series 4 were fitted to single-phase exponential decay models and the half-inhibition constants from each curve were tested against one another with a comparison of fits analysis. In Series 5, $J^{Na}{}_{in}$ and $J^{K}{}_{net}$ data were evaluated against Michaelis-Menten and linear regression models and the most appropriate fit was determined for each treatment; differences in J_{max} and K_m parameters for $J^{Na}{}_{in}$ data were tested using a comparison of fits analysis, while $J^{K}{}_{net}$ data were tested against the null hypothesis of slope = 0.

ACKNOWLEDGEMENTS

The authors thank Noah's Pet Ark for supplying zebrafish, Patrick Tamkee and Eric Lotto for help in the UBC-Zoology Aquatics Facility, Drs. Colin Brauner, Samuel Starko, Scott Parks and Alex Zimmer for data discussions, and to the three anonymous referees for their thoughtful and constructive reviews.

CONFLICTS OF INTEREST

The authors declare no competing interests.

DATA AVAILABILITY STATEMENT

The data that support the findings of this study are openly available on Dryad at https://doi.org/10.6076/D1KK5Z ref. (90).

ORCID

Alexander M. Clifford https://orcid.org/0000-0002-2836-5832
Martin Tresguerres https://orcid.org/0000-0002-7090-9266
Greg G. Goss https://orcid.org/0000-0003-0786-8868
Chris M. Wood https://orcid.org/0000-0002-9542-2219

REFERENCES

1. Krogh A.*Osmotic Regulation in Aquatic Animals*. Cambridge: Cambridge University Press; 1939.
2. Maetz J. Na^+/NH_4^+, Na^+/H^+ exchanges and NH_3 movement across the gill of *Carassius auratus*. *J Exp Biol*. 1973;58(1):255-275.
3. Maetz J, Romeu FG. The mechanism of sodium and chloride uptake by the gills of a fresh-water fish, *Carassius auratus*: II. Evidence for NH_4^+/Na^+ and HCO_3^-/Cl^- exchanges. *J Gen Physiol*. 1964;47(6):1209-1227.
4. Wright PA, Wood CM. A new paradigm for ammonia excretion in aquatic animals: role of Rhesus (Rh) glycoproteins. *J Exp Biol*. 2009;212(Pt 15):2303-2312.
5. Wu S-C, Horng J-L, Liu S-T, et al. Ammonium-dependent sodium uptake in mitochondrion-rich cells of medaka (*Oryzias latipes*) larvae. *Am J Physiol-Cell Physiol*. 2009;298(2):C237-C250.
6. Nakada T, Hoshijima K, Esaki M, Nagayoshi S, Kawakami K, Hirose S. Localization of ammonia transporter Rhcg1 in mitochondrion-rich cells of yolk sac, gill, and kidney of zebrafish and its ionic strength-dependent expression. *Am J Physiol-Regul Integr Comp Physiol*. 2007;293(4):R1743-R1753.
7. Nawata CM, Hung CCY, Tsui TKN, Wilson JM, Wright PA, Wood CM. Ammonia excretion in rainbow trout (*Oncorhynchus mykiss*): evidence for Rh glycoprotein and H^+-ATPase involvement. *Physiol Genomics*. 2007;31(3):463-474.
8. Dymowska AK, Schultz AG, Blair SD, Chamot D, Goss GG. Acid-sensing ion channels are involved in epithelial Na^+ uptake in the rainbow trout *Oncorhynchus mykiss*. *Am J Physiol-Cell Physiol*. 2014;307(3):C255-C265.
9. Dymowska AK, Boyle D, Schultz AG, Goss GG. The role of acid-sensing ion channels in epithelial Na^+ uptake in adult zebrafish (*Danio rerio*). *J Exp Biol*. 2015;218(8):1244-1251.
10. Avella M, Bornancin M. A new analysis of ammonia and sodium transport through the gills of the freshwater rainbow trout (*Salmo gairdneri*). *J Exp Biol*. 1989;142:155-217.
11. Wilson JM, Randall DJ, Donowitz M, Vogl AW, Ip AK. Immunolocalization of ion-transport proteins to branchial epithelium mitochondria-rich cells in the mudskipper (*Periophthalmodon schlosseri*). *J Exp Biol*. 2000;203(Pt 15):2297-2310.
12. Sullivan G, Fryer J, Perry S. Immunolocalization of proton pumps (H^+-ATPase) in pavement cells of rainbow trout gill. *J Exp Biol*. 1995;198(12):2619-2629.
13. Kwong RWM, Perry SF. A role for sodium-chloride cotransporters in the rapid regulation of ion uptake following acute environmental acidosis: new insights from the zebrafish model. *Am J Physiol-Cell Physiol*. 2016;311(6):C931-C941.
14. Wu Shu-Chen, Horng Jiun-Lin, Liu Sian-Tai, et al. Ammonium-dependent sodium uptake in mitochondrion-rich cells of medaka (*Oryzias latipes*) larvae. *Am J Physiol-Cell Physiol*. 2010;298(2):C237–C250.
15. Yang T, Huang YG, Singh I, Schnermann J, Briggs JP. Localization of bumetanide- and thiazide-sensitive Na-K-Cl cotransporters along the rat nephron. *Am J Physiol-Ren Physiol*. 1996;271(4):F931-F939.
16. Jacquillet G, Rubera I, Unwin RJ. Potential role of serine proteases in modulating renal sodium transport *in vivo*. *Nephron Physiol*. 2011;119(2):p22-p29.
17. Hirata T, Kaneko T, Ono T, et al. Mechanism of acid adaptation of a fish living in a pH 3.5 lake. *Am J Physiol-Regul Integr Comp Physiol*. 2003;284(5):R1199-R1212.
18. Esaki M, Hoshijima K, Kobayashi S, Fukuda H, Kawakami K, Hirose S. Visualization in zebrafish larvae of Na^+ uptake in mitochondria-rich cells whose differentiation is dependent on foxi3a. *Am J Physiol-Regul Integr Comp Physiol*. 2007;292(1):R470-R480.
19. Yan J-J, Chou M-Y, Kaneko T, Hwang P-P. Gene expression of Na^+/H^+ exchanger in zebrafish H^+-ATPase-rich cells during acclimation to low-Na^+ and acidic environments. *Am J Physiol-Cell Physiol*. 2007;293(6):C1814-C1823.
20. Parks SK, Tresguerres M, Goss GG. Theoretical considerations underlying Na^+ uptake mechanisms in freshwater fishes. *Comp Biochem Physiol C-Toxicol Pharmacol*. 2008;148(4):411-418.
21. Engeszer RE, Patterson LB, Rao AA, Parichy DM. Zebrafish in the wild: a review of natural history and new notes from the field. *Zebrafish*. 2007;4(1):21-40.
22. Shamshuddin J, Panhwar QA, Alia FJ, Fauziah CI. Formation and utilisation of acid sulfate soils in Southeast Asia for sustainable rice cultivation. *Trop Agric Sci*. 2017;40(2):225-246.

23. Morales LA, Paz-Ferreiro J, Vieira SR, Vázquez EV. Spatial and temporal variability of Eh and pH over a rice field as related to lime addition. *Bragantia*. 2010;69:67-76.
24. Azura A, Shamshuddin J, Fauziah CI. Root elongation, root surface area and organic acid by rice seedling under Al^{3+} and/or H^+ stress. *Am J Agric Biol Sci*. 2011;6(3):321-331.
25. Shamshuddin J, Elisa AA, Ali R, Fauziah I. Rice defense mechanisms against the presence of excess amount of Al^{3+} and Fe^{2+} in the water. *Aust J Crop Sci*. 2013;7(3):314-320.
26. Alia FJ, Shamshuddin J, Fauziah CI, Husni MHA, Panhwar QA. Effects of Aluminum, Iron and/or low pH on rice seedlings grown in solution culture. *Int J Agric Biol*. 2015;17(4):702-710.
27. Sundin J, Morgan R, Finnøen MH, Dey A, Sarkar K, Jutfelt F. On the observation of wild zebrafish (*Danio rerio*) in India. *Zebrafish*. 2019;16(6):546-553.
28. Lewis L, Kwong RWM. Zebrafish as a model system for investigating the compensatory regulation of ionic balance during metabolic acidosis. *Int J Mol Sci*. 2018;19(4):1087.
29. Kumai Y, Perry SF. Ammonia excretion via Rhcg1 facilitates Na^+ uptake in larval zebrafish, *Danio rerio*, in acidic water. *Am J Physiol-Regul Integr Comp Physiol*. 2011;301(5):R1517-R1528.
30. Kumai Y, Bernier NJ, Perry SF. Angiotensin-II promotes Na^+ uptake in larval zebrafish, *Danio rerio*, in acidic and ion-poor water. *J Endocrinol*. 2014;220(3):195-205.
31. Caner T, Abdulnour-Nakhoul S, Brown K, Islam MT, Hamm LL, Nakhoul NL. Mechanisms of ammonia and ammonium transport by rhesus-associated glycoproteins. *Am J Physiol-Cell Physiol*. 2015;309(11):C747-C758.
32. Zimmer AM, Shir-Mohammadi K, Kwong RWM, Perry SF. Reassessing the contribution of the Na^+/H^+ exchanger Nhe3b to Na^+ uptake in zebrafish (*Danio rerio*) using CRISPR/Cas9 gene editing. *J Exp Biol*. 2020;223:jeb215111.
33. Chang W-J, Wang Y-F, Hu H-J, Wang J-H, Lee T-H, Hwang P-P. Compensatory regulation of Na^+ absorption by Na^+/H^+ exchanger and Na^+-Cl^- cotransporter in zebrafish (*Danio rerio*). *Front Zool*. 2013;10(1):46.
34. Kleyman TR, Cragoe EJ. Amiloride and its analogs as tools in the study of ion transport. *J Membr Biol*. 1988;105(1):1-21.
35. Boyle D, Clifford AM, Orr E, Chamot D, Goss GG. Mechanisms of Cl^- uptake in rainbow trout: Cloning and expression of slc26a6, a prospective Cl^-/HCO_3^- exchanger. *Comp Biochem Physiol -Mol Integr Physiol*. 2015;180:43-50.
36. Chen X, Qiu L, Li M, et al. Diarylamidines: high potency inhibitors of acid-sensing ion channels. *Neuropharmacology*. 2010;58(7):1045-1053.
37. Brix KV, Brauner CJ, Schluter D, Wood CM. Pharmacological evidence that DAPI inhibits NHE2 in *Fundulus heteroclitus* acclimated to freshwater. *Comp Biochem Physiol Part C Toxicol Pharmacol*. 2018;211:1-6.
38. Shih T-H, Horng J-L, Liu S-T, Hwang P-P, Lin L-Y. Rhcg1 and NHE3b are involved in ammonium-dependent sodium uptake by zebrafish larvae acclimated to low-sodium water. *Am J Physiol Regul Integr Comp Physiol*. 2012;302(1):R84-93.
39. Garvin JL, Simon SA, Cragoe EJ, Mandel LJ. Phenamil: An irreversible inhibitor of sodium channels in the toad urinary bladder. *J Membr Biol*. 1985;87(1):45-54.
40. Alvarez de la Rosa D, Canessa CM, Fyfe GK, Zhang P. Structure and regulation of amiloride-sensitive sodium channels. *Annu Rev Physiol*. 2000;62:573-594.
41. Reid SD, Hawkings GS, Galvez F, Goss GG. Localization and characterization of phenamil-sensitive Na^+ influx in isolated rainbow trout gill epithelial cells. *J Exp Biol*. 2003;206(Pt 3):551-559.
42. Giménez I. Molecular mechanisms and regulation of furosemide-sensitive Na–K–Cl cotransporters. *Curr Opin Nephrol Hypertens*. 2006;15(5):517.
43. Stokes J, Lee I, Damico M. Sodium-chloride absorption by the urinary-bladder of the winter flounder - a thiazide-sensitive, electrically neutral transport-system. *J Clin Invest*. 1984;74(1):7-16.
44. Beaumont K, Vaughn DA, Maciejewski AR, Fanestil DD. Reversible downregulation of thiazide diuretic receptors by acute renal ischemia. *Am J Physiol-Ren Physiol*. 1989;256(2):F329-F334.
45. Wang Y-F, Tseng Y-C, Yan J-J, Hiroi J, Hwang P-P. Role of SLC12A10.2, a Na-Cl cotransporter-like protein, in a Cl uptake mechanism in zebrafish (*Danio rerio*). *Am J Physiol-Regul Integr Comp Physiol*. 2009;296(5):R1650-R1660.
46. Horng J-L, Hwang P-P, Shih T-H, Wen Z-H, Lin C-S, Lin L-Y. Chloride transport in mitochondrion-rich cells of euryhaline tilapia (*Oreochromis mossambicus*) larvae. *Am J Physiol-Cell Physiol*. 2009;297(4):C845-C854.
47. Maren TH. Carbonic anhydrase: chemistry, physiology, and inhibition. *Physiol Rev*. 1967;47(4):595-781.
48. Yellen G. Permeation in potassium channels: Implications for channel structure. *Annu Rev Biophys Chem*. 1987;16(1):227-246.
49. Taglialatela M, Drewe JA, Brown AM. Barium blockade of a clonal potassium channel and its regulation by a critical pore residue. *Mol Pharmacol*. 1993;44(1):180-190.
50. Choe H, Sackin H, Palmer LG. Permeation properties of inward-rectifier potassium channels and their molecular determinants. *J Gen Physiol*. 2000;115(4):391-404.
51. Rubino JG, Wilson JM, Wood CM. An *in vitro* analysis of intestinal ammonia transport in fasted and fed freshwater rainbow trout: roles of NKCC, K^+ channels, and Na^+, K^+ ATPase. *J Comp Physiol B*. 2019;189:549-566.
52. Wu Z-Z, Li D-P, Chen S-R, Pan H-L. Aminopyridines potentiate synaptic and neuromuscular transmission by targeting the voltage-activated calcium channel β subunit. *J Biol Chem*. 2009;284(52):36453-36461.
53. Latorre R, Vergara C, Hidalgo C. Reconstitution in planar lipid bilayers of a Ca^{2+}-dependent K^+ channel from transverse tubule membranes isolated from rabbit skeletal muscle. *Proc Natl Acad Sci USA*. 1982;79(3):805-809.
54. Lang DG, Ritchie AK. Tetraethylammonium blockade of apamin-sensitive and insensitive Ca^{2+}-activated K^+ channels in a pituitary cell line. *J Physiol*. 1990;425:117-132.
55. Khodakhah K, Melishchuk A, Armstrong CM. Killing K channels with TEA+. *Proc Natl Acad Sci USA*. 1997;94(24):13335-13338.
56. Zemková H, Teisinger J, Vyskocil F. Inhibition of the electrogenic Na, K pump and Na, K-ATPase activity by tetraethylammonium, tetrabutylammonium, and apamin. *J Neurosci Res*. 1988;19(4):497-503.
57. Kim M-H, Korogod N, Schneggenburger R, Ho W-K, Lee S-H. Interplay between Na^+/Ca^{2+} exchangers and mitochondria in Ca^{2+} clearance at the Calyx of Held. *J Neurosci*. 2005;25(26):6057-6065.
58. Lee JS, Kim M-H, Ho W-K, Lee S-H. Developmental upregulation of presynaptic NCKX underlies the decrease of

mitochondria-dependent posttetanic potentiation at the rat calyx of Held synapse. *J Neurophysiol*. 2013;109(7):1724-1734.
59. Kumai Y, Bahubeshi A, Steele S, Perry SF. Strategies for maintaining Na^+ balance in zebrafish (*Danio rerio*) during prolonged exposure to acidic water. *Comp Biochem Physiol A Mol Integr Physiol*. 2011;160(1):52-62.
60. Brix KV, Grosell M. Comparative characterization of Na^+ transport in *Cyprinodon variegatus* and *Cyprinodon variegatus hubbsi*: a model species complex for studying teleost invasion of freshwater. *J Exp Biol*. 2012;215(7):1199-1209.
61. Tresguerres M, Clifford AM, Harter TS, et al. Evolutionary links between intra- and extracellular acid–base regulation in fish and other aquatic animals. *J Exp Zool Part Ecol Integr Physiol*. 2020;333(6):449-465.
62. Hwang PP, Lee TH. New insights into fish ion regulation and mitochondrion-rich cells. *Comp Biochem Physiol Part A*. 2007;148:479-497.
63. Kirschner LB. Water and ions. In: Prosser CL, ed. *Environmental and metabolic animal physiology*. 1991:13-107.
64. Wood CM, LeMoigne J. Intracellular acid-base responses to environmental hyperoxia and normoxic recovery in rainbow trout. *Respir Physiol*. 1991;86(1):91-113.
65. Morgan IJ, Potts WTW, Oates K. Intracellular ion concentrations in branchial epithelial cells of brown trout (*Salmo trutta* L.) determined by X-ray microanalysis. *J Exp Biol*. 1994;194(1):139-151.
66. García Romeu F, Maetz J. The mechanism of sodium and chloride uptake by the gills of a fresh-water fish, *Carassius auratus*. *J Gen Physiol*. 1964;47(6):1195-1207.
67. Gonzalez RJ, Wood CM, Wilson RW, et al. Effects of water pH and calcium concentration on ion balance in fish of the Rio Negro. *Amazon. Physiol Zool*. 1998;71(1):15-22.
68. Wilson RW, Wood CM, Gonzalez RJ, et al. Ion and acid-base balance in three species of Amazonian fish during gradual acidification of extremely soft water. *Physiol Biochem Zool*. 1999;72(3):277-285.
69. Evans DH. *Osmotic and Ionic Regulation: Cells and Animals*, 1st ed. CRC Press; 2008.
70. Wood CM, Bucking C. 5 - The role of feeding in salt and water balance. In: Grosell M, Farrell AP, Brauner CJ, eds. *Fish Physiology*. Academic Press; 2010:165-212.
71. Furukawa F, Watanabe S, Kimura S, Kaneko T. Potassium excretion through ROMK potassium channel expressed in gill mitochondrion-rich cells of Mozambique tilapia. *Am J Physiol-Regul Integr Comp Physiol*. 2011;302(5):R568-R576.
72. Neyton J, Miller C. Potassium blocks barium permeation through a calcium-activated potassium channel. *J Gen Physiol*. 1988;92(5):549-567.
73. Ma X-Y, Yu J-M, Zhang S-Z, et al. External Ba^{2+} block of the two-pore domain potassium channel TREK-1 defines conformational transition in its selectivity filter. *J Biol Chem*. 2011;286(46):39813-39822.
74. Judge SIV, Bever CT. Potassium channel blockers in multiple sclerosis: neuronal K_v channels and effects of symptomatic treatment. *Pharmacol Ther*. 2006;111(1):224-259.
75. He C, O'Halloran DM. Analysis of the Na^+/Ca^{2+} exchanger gene family within the phylum Nematoda. *PLoS One*. 2014;9(11):e112841.
76. Su YH, Vacquier VD. A flagellar K^+-dependent Na^+/Ca^{2+} exchanger keeps Ca^{2+} low in sea urchin spermatozoa. *Proc Natl Acad Sci USA*. 2002;99(10):6743-6748.
77. Sakurai K, Vinberg F, Wang T, Chen J, Kefalov VJ. The Na^+/Ca^{2+}, K^+ exchanger 2 modulates mammalian cone phototransduction. *Sci Rep*. 2016;6(1):32521.
78. Lamason RL, Mohideen M-APK, Mest JR, et al. SLC24A5, a putative cation exchanger, affects pigmentation in zebrafish and humans. *Science*. 2005;310(5755):1782-1786.
79. Hassan MT, Lytton J. Potassium-dependent sodium-calcium exchanger (NCKX) isoforms and neuronal function. *Cell Calcium*. 2020;86:102135.
80. Lee S-H, Kim M-H, Park KH, Earm YE, Ho W-K. K^+-dependent Na^+/Ca^{2+} exchange is a major Ca^{2+} clearance mechanism in axon terminals of rat neurohypophysis. *J Neurosci Off J Soc Neurosci*. 2002;22(16):6891-6899.
81. Altimimi HF, Schnetkamp PPM. Na^+/Ca^{2+}-K^+ exchangers (NCKX) - Functional properties and physiological roles. *Channels*. 2007;1(2):62-69.
82. Altimimi HF, Szerencsei RT, Schnetkamp PPM. Functional and structural properties of the NCKX2 Na^+/Ca^{2+}-K^+ exchanger: a comparison with the NCX1 Na^+/Ca^{2+} exchanger. *Adv Exp Med Biol*. 2013;961:81-94.
83. Yang H, Choi K-C, Jung E-M, An B-S, Hyun S-H, Jeung E-B. Expression and regulation of sodium/calcium exchangers, NCX and NCKX, in reproductive tissues: do they play a critical role in calcium transport for reproduction and development? *Adv Exp Med Biol*. 2013;961:109–121.
84. Schnetkamp PPM. The SLC24 gene family of Na^+/Ca^{2+}–K^+ exchangers: From sight and smell to memory consolidation and skin pigmentation. *Mol Aspects Med*. 2013;34(2-3):455-464.
85. Kwong RWM, Kumai Y, Perry SF. The physiology of fish at low pH: the zebrafish as a model system. *J Exp Biol*. 2014;217(Pt 5):651-662.
86. Gonzalez RJ, Patrick ML, Duarte RM, et al. Exposure to pH 3.5 water has no effect on the gills of the Amazonian tambaqui (*Colossoma macropomum*). *J Comp Physiol [B]*. 2021;191(3):493-502.
87. Morris C, Val AL, Brauner CJ, Wood CM. The physiology of fish in acidic waters rich in dissolved organic carbon, with specific reference to the Amazon basin: Ionoregulation, acid–base regulation, ammonia excretion, and metal toxicity. *J Exp Zool Part Ecol Integr Physiol*. 2021;335(9-10):843–863.
88. Dymowska AK, Hwang P-P, Goss GG. Structure and function of ionocytes in the freshwater fish gill. *Respir Physiol Neurobiol*. 2012;184(3):282-292.
89. Clifford AM, Weinrauch AM, Goss GG. Dropping the base: Recovery from extreme hypercarbia in the CO_2 tolerant Pacific hagfish (*Eptatretus stoutii*). *J Comp Physiol B*. 2018;188(3):421-435.
90. Clifford A, Tresguerres M, Goss G, Wood C. Dataset for 'A novel K^+-dependent Na^+ uptake mechanism during low pH exposure in adult zebrafish (*Danio rerio*): New tricks for old dogma', Dryad, Dataset, https://doi.org/10.6076.D1KK5Z.

How to cite this article: Clifford AM, Tresguerres M, Goss GG, Wood CM. A novel K^+-dependent Na^+ uptake mechanism during low pH exposure in adult zebrafish (*Danio rerio*): New tricks for old dogma. *Acta Physiol*. 2022;00:e13777. doi:10.1111/apha.13777